



One-Piece Dome Fabrication Study Final Report

Boeing Engineering & Construction

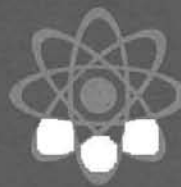
Prepared by Sandia Laboratories, Albuquerque, New Mexico 87115
and Livermore, California 94550 for the United States Department
of Energy under Contract DE-AC04-76DP00789.

Printed December 1979

*When printing a copy of any digitized SAND
Report, you are required to update the
markings to current standards.*



Sandia Laboratories
energy report



Issued by Sandia Laboratories, operated for the United States Department of Energy by Sandia Corporation.

NOTICE

This report was prepared as an account of work sponsored by the United States Government. Neither the United States nor the United States Department of Energy, nor any of their employees, nor any of their contractors, subcontractors, or their employees, makes any warranty, express or implied, or assumes any legal liability or responsibility for the accuracy, completeness or usefulness of any information, apparatus, product or process disclosed, or represents that its use would not infringe privately owned rights.

Printed in the United States of America
Available from
National Technical Information Service
U. S. Department of Commerce
5285 Port Royal Road
Springfield, VA 22161
Price: Printed Copy \$6.00; Microfiche \$3.00

**SAND78-8184
Unlimited Release
Printed December 1979**

ONE-PIECE DOME FABRICATION STUDY

FINAL REPORT

**Prepared For
Sandia Laboratories
Livermore, California**

**Under
Contract 18-7830**

by

**Boeing Engineering and Construction Company
A division of The Boeing Company
Seattle, Washington 98124**

BOEING DOCUMENT No. D180-25415-1

FOREWORD

This final report on the "One-Piece Dome Fabrication Study" is submitted in fulfillment of Sandia Contract 18-7830, Work Statement Task B-8. Results from both Phases A and B are included in the report. Sandia program management was provided by Mr. Clayton Mavis. Boeing engineering personnel contributing to the project included Messrs Frank Tipton, David Kirkbride, Marcus Berry, and Harry Dursch. Roger Gillette was project manager for Boeing Engineering and Construction (BEC).

NOTICE

This report was prepared as an account of work sponsored by the United States Government. Neither the United States nor the United States Department of Energy, nor any of their employees, nor any of their contractors, subcontractors, or their employees, makes any warranty, express or implied, or assumes any legal liability or responsibility for the accuracy, completeness or usefulness of any information, apparatus, product or process developed, or represents that its use would not infringe privately owned rights.

TABLE OF CONTENTS

		PAGE
1.0	INTRODUCTION AND SUMMARY	1
2.0	THERMOFORMING FACILITIES	4
2.1	PHASE A THERMOFORMING FACILITY	4
2.1.1	Heat Source Design	4
2.1.2	Controls and Instrumentation	6
2.2	PHASE B THERMOFORMING FACILITY	8
2.2.1	Preheater Assembly	8
2.2.2	Plenum/Aperture Assembly	8
2.2.3	Auxiliary Heater Array	11
2.2.4	Enclosure	11
2.2.5	Air Supply System	11
3.0	MATERIAL SELECTION	12
4.0	EXPERIMENTAL APPROACH	15
4.1	EXPERIMENTAL VARIABLES	15
4.2	FABRICATION PROCEDURES	16
5.0	PENNWALT THERMOFORMING EXPERIMENTS	20
5.1	INITIAL STUDY OF THERMOFORMING PARAMETERS	20
5.1.1	Twenty Percent Offset Yield	22
5.1.2	Break Strength	26
5.1.3	Transmission After Heat Ageing	26
5.1.4	Area Change After Heat Ageing	29
5.2	PHASE A KYNAR THERMOFORMING RESULTS (PENNWALT)	29
5.2.1	Process Experiments	29
5.2.2	Environmental Test Domes	35
5.3	PHASE B THERMOFORMING FACILITY (PENNWALT)	35
5.4	PHASE B KYNAR THERMOFORMING RESULTS (PENNWALT)	38
5.5	WEATHEROMETER TESTS	43
6.0	THERMOFORMING EXPERIMENTAL RESULTS	51
6.1	POLYVINYLIDENE FLUORIDE (KYNAR)	51
6.1.1	Kynar Process Experiment	51
6.1.2	Properties of Phase B Kynar Domes	52
6.2	POLYESTER (PETRA)	55
6.2.1	Polyester Process Experiment	55
6.2.2	Properties of Phase B Petra Domes	61

	PAGE
6.3	OTHER MATERIALS 65
6.3.1	Polyester (Meliform and Melinex-0) 65
6.3.2	Polyester (PETG 7821) 69
6.3.3	Cellulose Acetate Butyrate (UVEX) 69
6.3.4	Polyvinyl Fluoride (Tedlar) 69
6.3.5	Ethylene - Chlorotrifluoroethylene (Halar) 69
6.4	PREFORM PREPARATION 70
6.4.1	Heat Sealing Experiments 70
6.4.2	Lamination Experiments 71
6.4.3	Butt Welding Experiment 72
6.4.4	Wide Extrusions 72
7.0	DESERT EXPOSURE TESTS 73
7.1	APPARATUS 73
7.2	RESULTS OF DESERT EXPOSURE 73
8.0	FULL SCALE DOME CAPABILITY 86
9.0	CONCLUSIONS AND RECOMMENDATIONS 88

LIST OF FIGURES

<u>Figure</u>		<u>Page</u>
2.1-1	Phase A Thermoforming Facility	5
2.1-2	Phase A Thermoforming Apparatus Controls and Instrumentation	7
2.2-1	Phase B Thermoforming Facility	9
2.2-2	Phase B Thermoforming Facility Schematic	10
3.0-1	Comparative Film Thermal Properties	13
4.2-1	Typical Heat Flux and Temperature Cycle for Phase A Polyester Domes	17
4.2-2	Typical Pressure and Flow Variation During Forming for Phase A Polyester Domes	18
5.1.1-1	Schematic of the Definition of 20% Offset Yield	24
5.1.1-2	20% Offset Yield vs. Stretching Temperature for Kynar 460	25
5.1.2-1	Break Strength vs. Stretch Temperature for Kynar 460	27
5.1.3-1	% Transmission vs. Stretching Temperature for Kynar 460	28
5.1.4-1	% Area Change vs. Stretching Temperature for Kynar 460	30
5.3-1	Schematic of Pennwalt's Phase B Thermoforming Facility	37
5.3-2	Preform Holder and Air Diffuser	39
5.3-3	Pennwalt's Thermoforming Facility - Phase B	40
5.4-1	Effect of Infrared Heater Temperature on Kynar Heating Characteristics	41
5.4-2	Temperature Profile Across Diameter of the Preform (Infrared Heater Setting = 260°C)	42
5.5-1	Normalized 20% Offset Yield vs. Hours in the Weatherometer	47
5.5-2	Normalized Break Strength vs. Hours in the Weatherometer	48
5.5-3	Normalized Elongations vs. Hours in the Weatherometer	49
5.5-4	% Transmission vs. Hours in the Weatherometer	50
6.1.2-1	Thickness Distribution of a Phase B Kynar Thermoformed Dome (No. 1/5/17)	53

		<u>Page</u>
6.1.2-2	Specular Transmittance of Phase B Kynar Dome (No. 1/5/17) vs. Dome Position	54
6.1.2-3	Best Fit Circle Concentrically Traced Over a Profile of a Phase B Kynar Dome (No. 1/5/15)	57
6.1.2-4	Deviation of Phase B Kynar Dome From a True Sphere Measured in % (No. 1/5/15)	58
6.2.1-1	Calculated and Measured Stretch Ratios and Film Thickness Distribution for Polyester Dome Formed in Phase A	62
6.2.2-1	Thickness Distribution of a Phase B Petra AXB Ther- moformed Dome (No. 3/5/21)	63
6.2.2-2	Transmittance of Phase B Petra AXB Dome (No. 3/5/21)	66
6.2.2-3	Best Fit Circle Concentrically Traced Over a Profile of a Phase B Petra AXB Dome (No. 1/5/22)	67
6.2.2-4	Deviation of Phase B Petra AXB Dome From a True Sphere Measured in % (No. 1/5/22)	68
7.1-1	Enclosure and Support Stand	75
7.1-2	Photograph of Enclosures and Support Stand	76
7.1-3	Photograph of Domes and Test Hardware	77

LIST OF TABLES

<u>Table</u>		<u>Page</u>
3.0-1	Thermoforming Materials	14
5.1-1	Tensile Testing for Radial Symmetry in Biaxially Oriented Film	20
5.1-2	16 Run Statistical Design	21
5.1-3	Results of the 16 Run Experimental Design (Properties Before and After Heat Ageing 70 Hours at 60°C)	23
5.2.1-1	Summary of Thermoformed Runs in Boeing Phase A Facility	31
5.2.1-2	Tensile Data of Selected Domes Formed in Boeing Phase A Facility	32
5.2.1-3	Summary of Data on Kynar 460 61 cm (24 in) Domes	34
5.2.2-1	Kynar Domes - Mechanical Properties	36
5.5-1	Tensile Testing of Kynar - Tedlar (Central and After 558.8 Hours of Weatherometer Exposure)	45
5.5-2	Transmission Before and After Accelerated Weathering	46
6.1.2-3	Mechanical Properties of Phase B Kynar Dome (No. 1/5/17)	56
6.2.1-1	Effect of Strain Rate on Tensile Properties of Polyester Dome	60
6.2.2-1	Mechanical Properties of Phase B Petra AXB Dome (No. 3/5/21)	64
7.0-1	Environmental Exposure Test Materials	74
7.2-1	Mechanical Properties of a Phase A Petra AXB Dome with a Heat-Sealed Joint Before and After Desert Exposure	79
7.2-2	Mechanical Properties of a Phase A Petra AXB Dome Before and After Desert Exposure	80

		<u>Page</u>
7.2-3	Mechanical Properties of a Phase A PETG 7821 Dome Before and After Desert Exposure	81
7.2-4	Mechanical Properties of a Phase A Meliform Dome Before and After Desert Exposure	82
7.2-5	Mechanical Properties of a Phase A Petra AXB Laminated 4-Ply Butt Joint Before and After Desert Exposure	83
7.2-6	Transmittance of Dome Materials Exposed 5 Months (53,600 Langleys) in Desert	84

1.0 INTRODUCTION AND SUMMARY

Thermoforming techniques were investigated for forming a heliostat enclosure in one continuous operation from a flat film blank. The objective was to develop low cost manufacturing processes using preferred materials, and to provide scale-up data that will lead to full-scale dome production. Environmental tests have been initiated using formed small domes to determine the life expectancy of such domes.

Phase A used a modified existing facility to investigate the forming capability of various materials into small domes less than 76 cm (30 inches) in diameter. Materials and process variables were evaluated, the feasibility of various blank preparation techniques were verified, and environmental exposure tests were initiated. Phase A also included a subcontract with Pennwalt Corporation on thermoforming of polyvinylidene fluoride (Kynar). This contract was continued through Phase B.

The variables explored in Phase A included heat distribution during forming, air pressure and flow-rate profiles, expansion ratios, pre-heat time and temperature, and blowing time. The heat distribution was varied during forming to determine its effect on shape and thickness uniformity. Both uneven heating and radiant cooling were found to effect geometry. Pressure and flow variations, and blowing times were found to both effect shape and strength. Relatively high flow rates and pressure were required to obtain satisfactory properties. The strain rate required for good small domes is approximately 300%/minute. Expansion ratios up to 27 were investigated. The high expansion domes were found to have properties comparable to the normal domes with 6.8 expansion ratios. The pre-heat time and temperature were found to be significant in controlling the blowing pressure. The hotter the film, the lower the pressure required to form the dome. With some materials there was a problem of crystal growth when heated for too long a time. This crystallization caused opaqueness in the film and changes in mechanical properties.

In Phase A, Pennwalt performed a series of biaxial stretching experiments on flat film Kynar. A stretching machine, operated under a simultaneous two direction stretching mode, simulated the biaxial stretching experienced by the pole of a

thermoformed dome. This work was carried out as a fractional factorial experiment incorporating principles of statistical design. Seven variables were characterized quantitatively in terms of their influence on six final product properties, including the effect of thermal aging on stability. Using the information thus obtained it was possible to specify preform preparation and thermoforming parameters that would optimize the dome's properties.

Phase B continued the thermoforming experiments working with larger domes. Facilities capable of forming domes 1.22 m (4 ft) and 1.8 m (6 ft) in diameter were fabricated, preform preparation techniques applicable to full-scale domes were developed, and the desert exposure tests were continued. The materials investigated were Kynar and polyester (Petra). The Kynar thermoforming experiments were performed at both Pennwalt and BEC. The former investigated forming parameters utilizing a radiant heat facility capable of making 1.22 m (4 ft) diameter domes. The latter investigated scale-up feasibility and process parameters utilizing a facility which simulates processes in a full scale facility. Polyester domes with a nominal diameter up to 1.8 m (6 ft) and Kynar domes up to 1.4 m (4.5 ft), were made in the scale-up studies at BEC.

The Kynar domes formed in Phase B had excellent mechanical properties and adequate shape and thickness variations. The transmittance was low for those domes formed with material that was not quenched after extrusion. Domes formed with quenched material in Phase A had excellent transmittance.

The 1.8 m (6 ft) diameter Petra AXB dome formed in Phase B was the largest dome formed in this study. It was very spherical and had yield strengths and transmittance comparable to the better Phase A domes. The strengths were below the design requirements because the maximum thickness of preform material available for this study was only 0.5 mm (20 mils).

Satisfactory Kynar preforms were made using butt weld joints and press laminations. Both of these techniques along with overlapping heat seals are considered feasible for full scale 9.7 m (31.8 ft) diameter dome production. The overlapping heat seals with polyester were not as successful due to localized crystal growth with some of the polyester. The preforms laminated using vacuum did partially fuse but the air was not completely removed. Preforms made using both of these techniques were formed into satisfactory domes.

In Phase B, samples of Kynar from 3 domes fabricated in Phase A and a sample of polished Tedlar 400 SG (EXP) TR were exposed for over 500 hours in a carbon arc weatherometer. On the basis of short term correlations, this is equivalent to 16 to 28 years outdoor exposure. The Tedlar became brittle and hazy, losing approximately 90% of its elongation and 50% of its transmission. The Kynar lost 10 to 30% of its elongation and only 2 to 5% of its transmission.

In the desert exposure tests, 26 domes representing 9 different types were exposed at the Desert Sunshine Exposure Test Facility. The schedule for removal and test is 5, 12 and 18 months. The first samples after 5 months exposure were removed and tested. All of these were polyester. In general, the unstabilized polyesters, Meliform and PETG 7821, showed a substantial reduction in elongation, a slight increase in yield strength, and very little change in transmittance. The greatest elongation drop was noted in the heat sealed seam areas. The stabilized Petra AXB domes showed little change in the mechanical properties and only the 4 ply laminate dome showed any significant change in transmittance. The Kynar domes were not tested because the two domes being exposed were saved for the 12 and 18 month tests.

2.0 THERMOFORMING FACILITIES

Several thermoforming facilities were used to form domes in this study. In Phase-A, 0.36 m (1.18 ft) diameter domes were formed in a modified infrared oven. Most of the process development was carried out in this facility. For Phase B a larger facility, capable of forming domes up to 1.83m (6 ft) in diameter, was constructed at Boeing to evaluate scale up parameters. Pennwalt, in subcontract activities, utilized a hot air oven for Phase A thermoforming experiments on Kynar, and fabricated a radiant heat facility for Phase B. The latter was capable of forming domes up to 1.2 m (4 ft) diameter. A description of each of these facilities follows.

2.1 PHASE A THERMOFORMING FACILITY

An existing 1.2 m (4 ft) square infrared oven was modified to provide the thermoforming facility. An overall view is shown in Figure 2.1-1. The modifications consisted of adding auxiliary heat lamps, a preform holding fixture, and an air supply for blowing the domes. A 25.4 cm (10 in) diameter preform was selected for the experimental domes. This provided domes 35.8 cm (14.1 in) in diameter when blown to a base angle of 45° . This is equivalent to an area expansion ratio of 6.8. The maximum diameter that could be blown is around 76 cm (30 in) with an expansion ratio a little over 30.

The infrared heat chamber consisted of steel walls coated on the inside with a reflective coating. The blank holding fixture was an aluminum plate to which an aluminum ring was attached with clamps. The film to be formed was held between the plate and the ring. Fiberglass cloth was used under the film to diffuse the pressurized blowing air. This air was supplied to the middle of the bottom plate through 0.64cm (0.25 in) I.D. copper tubing .

2.1.1 Heat Source Design

The existing infrared heating source consisted of sixteen, 500 watt G-30 infrared heat lamps. These were mounted in a reflector frame that would be raised or lowered to vary the distance from the blank. They were controlled through a variable voltage power supply. Eight auxiliary heat lamp reflectors were added around the periphery of the blank holder. These each contained two 500-watt T-3 bulbs. These lamps were also controlled by a variable voltage power supply.

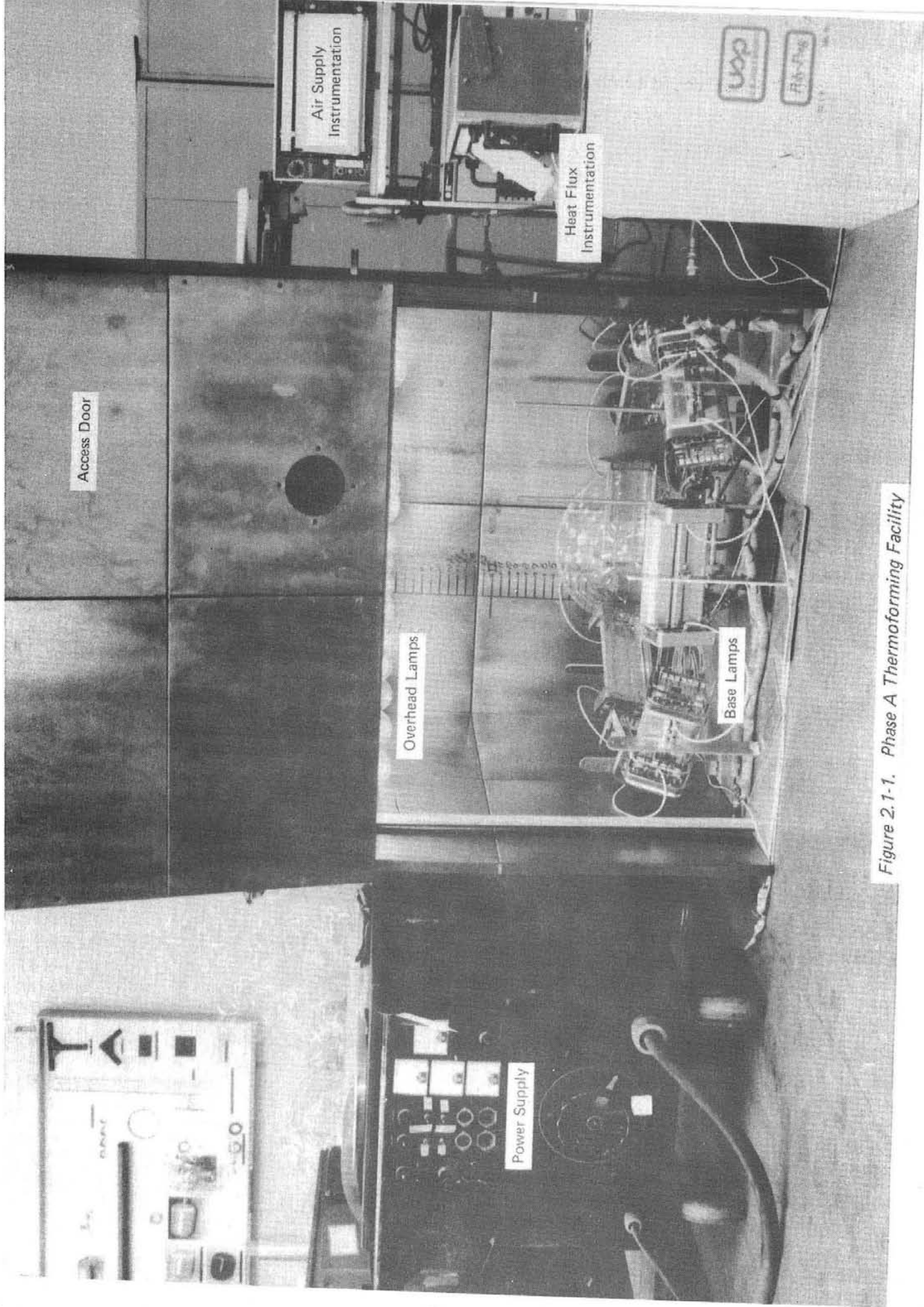


Figure 2.1-1. Phase A Thermoforming Facility

The thermal input could be varied by; physical movement of the heat lamps, changing voltage input to each lamp bank, or turning off selected groups of overhead lamps. The auxiliary lamp flux could also be varied by use of reflector shields.

2.1.2 Controls and Instrumentation

A general view of the controls and instrumentation used with the facility is shown in Figure 2.1-2. The air used in forming the domes was plant air controlled by a series of valves to obtain desired flow rates and pressures. The main flow control valve utilized a calibrated orifice to control and measure flow. A given flow rate was readily controlled, but constant pressure could only be maintained within limited conditions during forming. This was primarily caused by the fact that pressure was measured at the base of blank holder and represents the actual pressure exerted against the dome during forming. The resistance of the dome to this pressure will vary with size of the dome as well as the strength of the film. Another factor was the limited flow available through the pressure regulators at pressures below 35.5 kPa (5 psi). To cover the range of flows utilized, two different orifice sizes were required. One covered the range of 0 to 0.03m³/min (0 to 1 CFM), and the other from 0.03 to 0.3m³/min (1 to 10 CFM). The lower flow allowed the forming of a dome in approximately 2 minutes which was considered a reasonable forming time for full scale domes. At the higher flow rates a dome could be formed in 10 seconds. These higher forming rates increased the strain rates of the material and resulted in increased strength.

The radiant heat flux available was measured and recorded using calorimeters. These were positioned in the oven adjacent to and in the same plane as the film to obtain the heat flux input available to the film. The temperature of the film was measured by both thermocouples and an infrared pyrometer. Both of these were relative temperatures and were used for process control and repeatability. The thermocouples were positioned between two plies of film clamped together in a small frame and mounted on the blank holding fixture. The frame holding the thermocouple temperatures tended to lag behind the pyrometer readings.

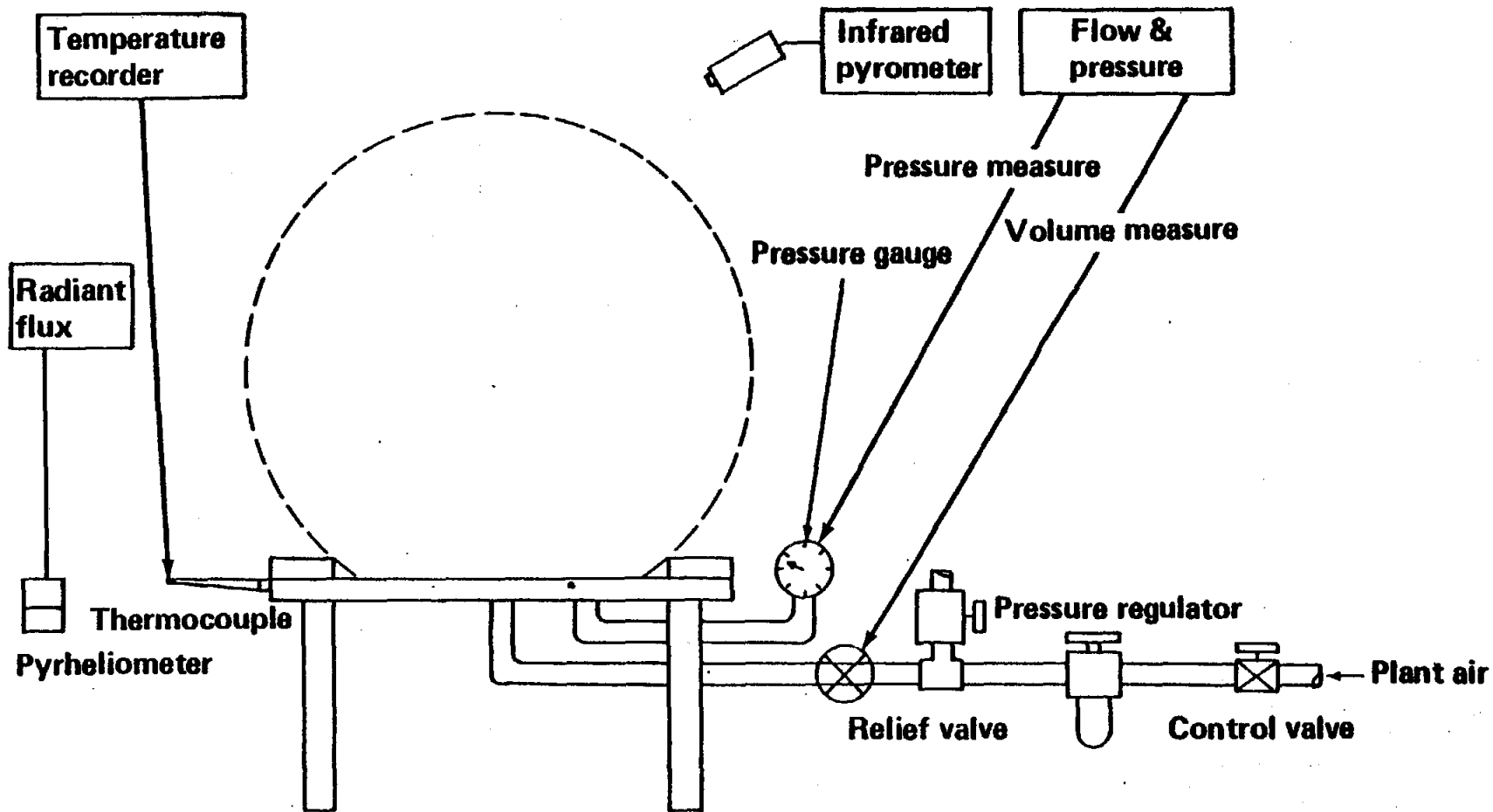


Figure 2.1-2. Phase A Thermoforming Apparatus Controls and Instrumentation

2.2 PHASE B THERMOFORMING FACILITY

The thermoforming facility used for Phase B experiments is shown in Figure 2.2-1. It consists of five major components; the preheater assembly, the plenum/aperture assembly, the auxiliary heater array, the enclosure and the air supply system. The facility was set up for manual operation to demonstrate the sequence of automated production. No special attention was given to environmental control of ambient conditions.

2.2.1 Preheater Assembly

The preheater assembly is shown schematically in Figure 2.2-2. It consists of twelve 0.46 m (18 in) wide by 0.5 m (36 in) long infrared heat source panels. These panels are wired to a time/temperature proportioning controller which regulates the 480 volt 3 phase power source. The heater panels are mechanically fastened to the assembly frame which utilizes track rollers to position the preheaters over the plenum/aperture assembly during preheat. Four machine screw studs allow vertical adjustment of the preheater height.

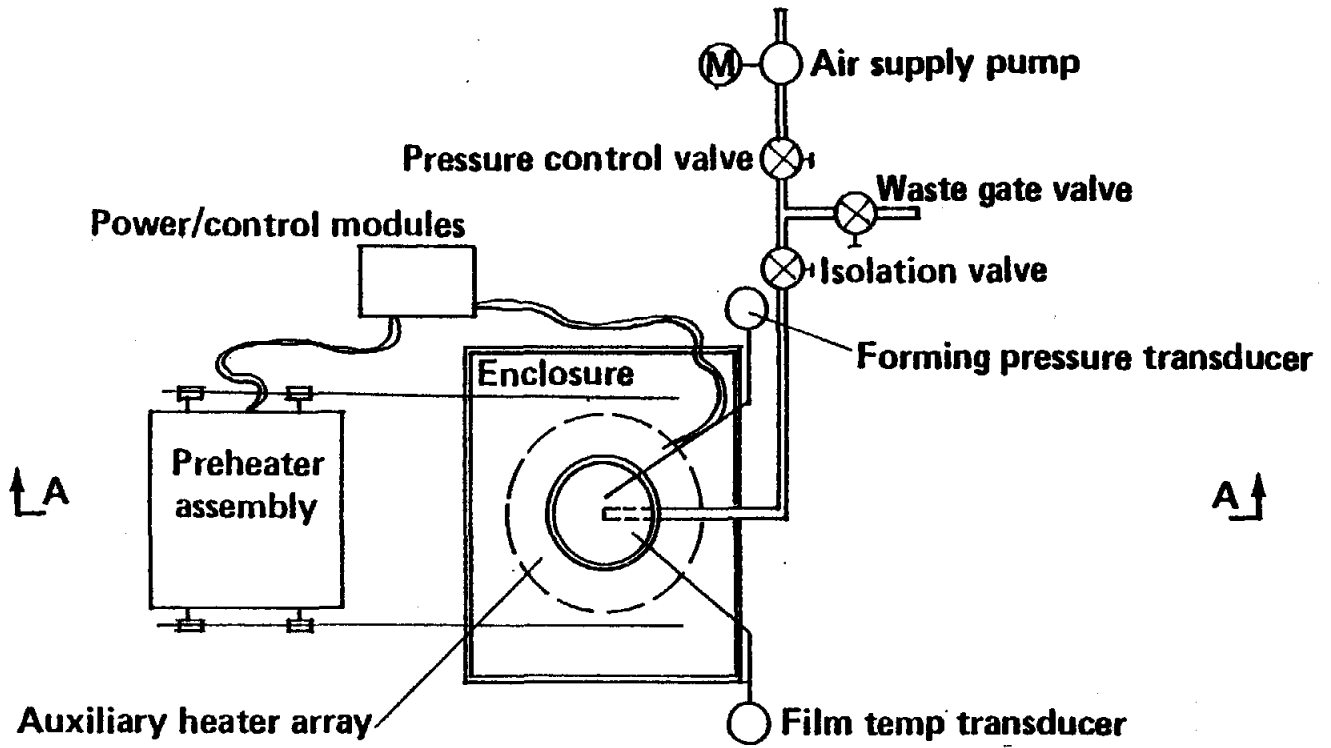
2.2.2 Plenum/Aperture Assembly

The plenum/aperture assembly is shown in Figure 2.2-2. The aperture ring is made up of four 90° arc sections. The inside radius of these arc sections is formed by a 25.4 mm (1.0 in) diameter pipe. In the clamped position these sections provide an aperture opening of 1.1 m (42.0 in). The bottom edge of a thermoformed enclosure has a 12.7 mm (1/2 in) radius molded into it as a result of the 25.4 mm (1.0 in) pipe.

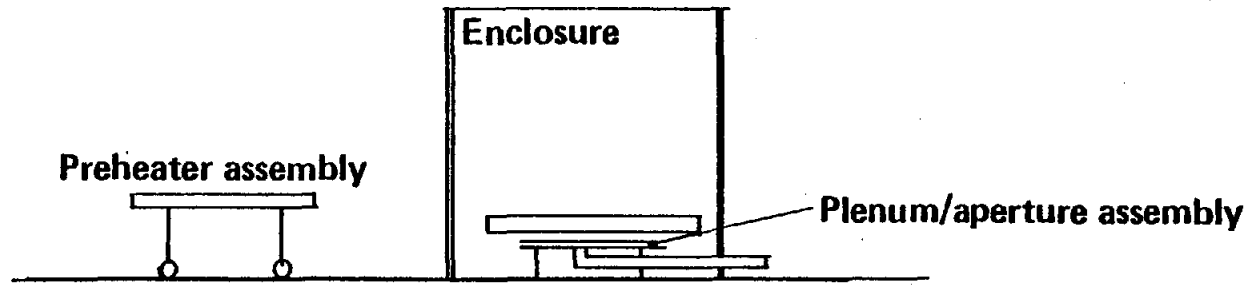
The plenum consists of a steel plate with a 152 mm (6.0 in) diameter hole machined through it. A steel pipe elbow welded to the back side of the plate connects the hole with the air supply system. An additional drilled and tapped hole in the plate accommodates a pressure transducer tap to monitor forming pressure.



Figure 2.2-1. Phase B Thermofforming Facility



PLAN VIEW
Thermoforming Facility



Section A-A

Figure 2.2-2. Phase B Thermoforming Facility Schematic

2.2.3 Auxiliary Heater Array

The auxiliary heater array shown in Figure 2.2-2 consisted of 19 heat lamp reflectors with two 500-watt T-3 bulbs each. These units were positioned on a 1.9 m (76 in) diameter circle around the plenum. A variable voltage power supply controlled their output intensity.

2.2.4 Enclosure

The primary purpose of the enclosure was to provide a safety shield during thermoforming. It was constructed by nailing corrugated aluminum panels to a wood frame. Openings were left on the top and a 1.2 m (4 ft) high by 3.6 m (12 ft) entrance/exit opening in one wall through which the preheater assembly was rolled.

2.2.5 Air Supply System

A diagram of the air supply system is shown in Figure 2.2-2. A constant displacement, low pressure blower capable of delivering $15.7 \text{ m}^3/\text{min}$ (560 CFM) of air at zero pressure head, supplied the air. Control of the system pressure/flow characteristics was accomplished by manual manipulation of the waste gate valve and pressure control valve. After forming, the isolation valve was closed to maintain air pressure in the finished thermoformed enclosure until cooled.

3.0 MATERIAL SELECTION

Principal requirements for plastic films considered for thermoforming are: thermoplastic; high specular transmittance after forming; long-term environmental stability; adequate strength; readily available in useful sizes and thicknesses; relatively inexpensive. The types that appear to be most promising are polyethylene terephthalate, polyvinylidene fluoride, polyvinyl fluoride, and ethylene-chlorotrifluoroethylene.

A chart of the comparative thermal properties of these materials is shown in Figure 3.0-1. The glass transition temperature (T_g), the thermoforming range, the crystalline melt temperature (T_m), and the heat sealing range is given where known. The material design requirements established for a formed dome are: specular transmittance equal to 86% minimum at a 0.14° cone angle and normal incidence; and strength equal to 5.78 kN/M (33 lbs/in) yield and 9.63 kN/M (55 lbs/in) ultimate.

The materials studied by Boeing in Phase A included 3 fluorocarbons, 3 polyesters, and a butyrate. These are listed in Table 3.0-1 along with their trade names, suppliers, and thickness. Pennwalt investigated Kynar 460 and Kynar 900 in their Phase A studies.

These Phase A materials were selected on the basis of an industry survey, a literature review, and the basic enclosure requirements. Some of them have inherent environmental resistance while others must have stabilizers added to improve resistance. They cover a price range of relatively inexpensive (\$2/kg) to very expensive (\$33/kg). All of them have absorptance bands in the infrared range allowing them to be heated by infrared heat lamps.

The materials investigated by Boeing in Phase B were limited to Kynar 460 (in thicknesses of 0.25 mm and 1.52 mm) and Petra AXB (0.51 mm thick). Pennwalt conducted thermoforming experiments on Kynar 460 in Phase B.

Comparative Film Thermal Properties

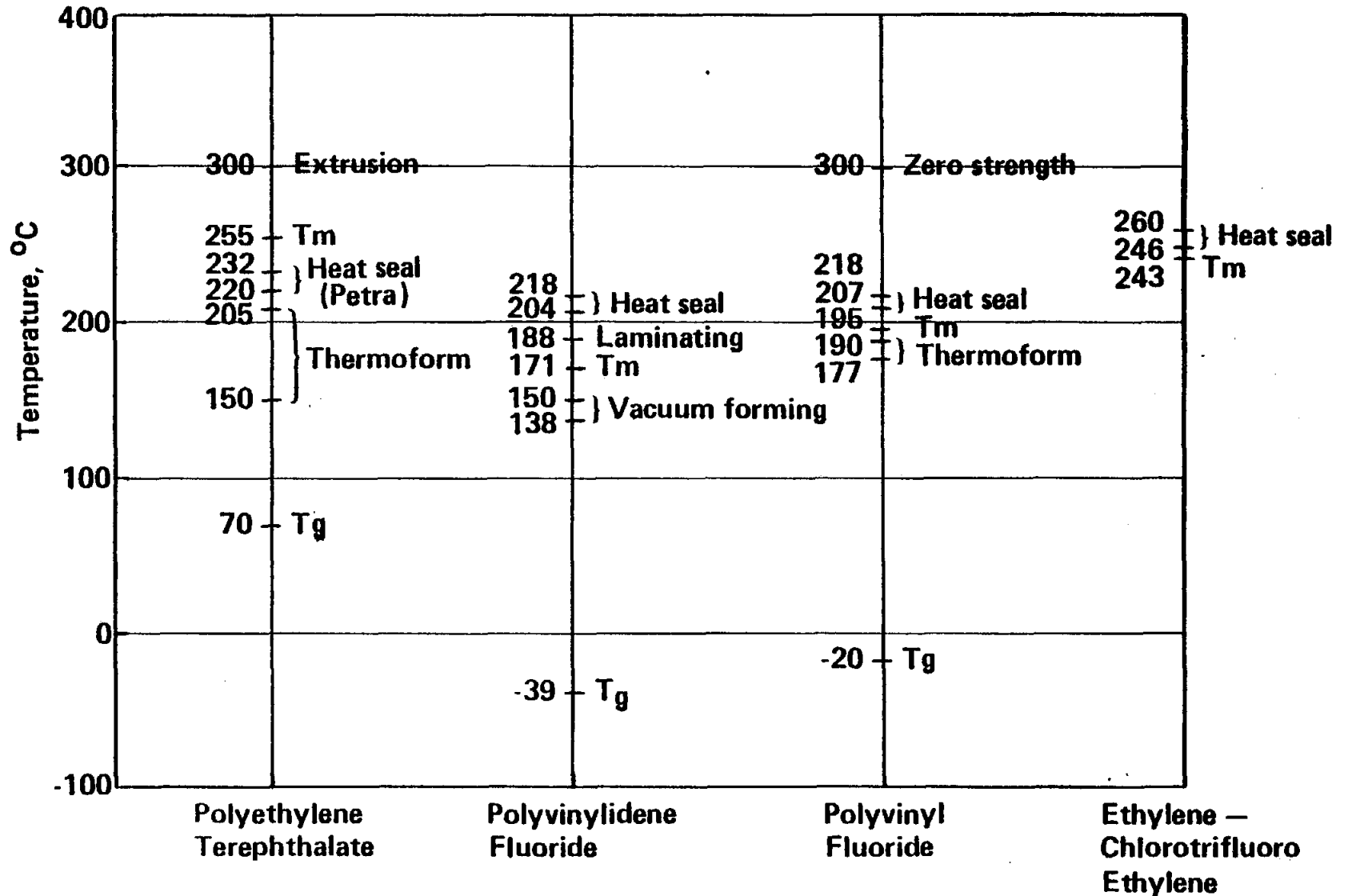


Figure 3.0-1. Comparative Film Thermal Properties

<u>Material (Supplier)</u>	<u>Thickness</u>
Fluoro Carbons	
PVF ₂ – Kynar (Pennwalt)	.051mm to 1.5mm (2 to 60 mils)
PVF – Tedlar 150-TRMF (Dupont)	.03mm (1.5 mil)
E-CTFE – Halar (Chemplast)	.127mm & .254mm (5 & 10 mils)
Polyester (PET)	
Petra A and AXB (Allied)	.127mm to .51mm (5 to 20 mils)
Meliform & Melinex-O (ICI)	.127mm to 1.27mm (5 to 50 mils)
PETG 7821 (Eastman Chemical)	.51mm (20 mils)
Cellulose Acetate Butyrate	
Uvex (Tennessee Eastman)	6.35mm (250 mils)

Table 3.0-1. Thermoforming Materials

4.0 EXPERIMENTAL APPROACH

The approach to thermoforming one piece enclosures was to combine standard thermoforming techniques with film orientation. The spherical shape was obtained by simply blowing a preheated sheet of film (preform). The orientation was developed by the high expansion ratios (on the order of 260% elongation for a 45° base angle dome) required to form an enclosure from a flat blank. This orientation is a means of improving the strength and durability of the film. In general these properties will be improved the most if: (1) the material is initially amorphous, (2) the material is stretched at the lowest practical temperature above T_g (glass transition temperature), and (3) stretched at the fastest rate possible. The primary limiting factor is that the material cannot be stretched at a rate that exceeds its strength at the temperature of stretching. Another critical requirement for both shape and property retention is rapid cooling after forming. Normal thermoforming variables, as well as orientation changes, were investigated by varying heating, forming, and cooling steps during the forming cycle.

4.1 EXPERIMENTAL VARIABLES

The primary variables in both Phase A and Phase B were; control of the "preform" preheating, and the air used to form the dome. The auxiliary (side lamp) heating and the cooling steps were varied slightly in Phase A but not at all in Phase B. Phase B domes were much larger than the Phase A domes, having a base diameter of 107 cm (42 in) compared to 25 cm (10 in) used in Phase A.

In the preform heating step the rate of heating was controlled by varying the power to the primary heaters and by varying their distance to the material. The final temperature was controlled by the heating time. The heat source temperature could be varied with both the heat lamps used in Phase A, and the infrared panels used in Phase B. This source temperature variation also controlled the wavelength of the radiant energy being emitted. At lower power settings, lamps radiated at a longer wavelength.

Air used to form the dome was regulated in pressure and flow rate to obtain controlled strain rates of the film. The volume of air used determined the final size of the dome. In both Phase A and B, the air supply systems used controls that did not

allow the pressure to be regulated independently of the flow rate. This resulted in a maximum pressure being provided to the dome forming cavity for any given flow rate.

This was not necessarily the pressure exerted on the film. The temperature of the film, dome geometry, and the amount of orientation determined the pressure required to expand the film. Because of this, for a given flow rate, the pressure varied during the forming step. To form a dome at constant pressure would require that the flow rate change as the dome is formed.

In Phase A the cooling step consisted of a quick shutdown of the lamps and opening the door (one entire side of the chamber). In Phase B, only the shutdown of the auxiliary lamps was used.

4.2 FABRICATION PROCEDURES

The initial fabrication step was to prepare the preform. This typically consisted of trimming the film to shape and mounting it in the fixture. For preforms with heat-sealed joints, the joints were made prior to trimming. For the laminated preforms used in Phase A, the various plies were positioned and bagged using the top ply as the bag. The laminant was then put under vacuum and fused using the infrared oven. The fused laminant was then trimmed and mounted. The laminated preforms used in Phase B were press laminated prior to trimming and mounting.

The forming cycle consisted of three steps; heating, forming, and cooling. A typical heat flux and temperature profile used for forming polyester domes in Phase A, is shown in Figure 4.2-1. Corresponding air flow and pressure changes are shown in Figure 4.2-2. Similar curves were obtained during Phase B experiments except that the heating cycle times were generally shorter and pressures were lower. For example, Phase B experiments Kynar was heated in approximately 2.5 minutes, and the polyester in 1 to 1.5 minutes.

In general, during the heating step the measured radiant energy rose slowly after the initial increase when the lamps were turned on or the infrared heaters were positioned over the sample. The heating step was continued until the reference

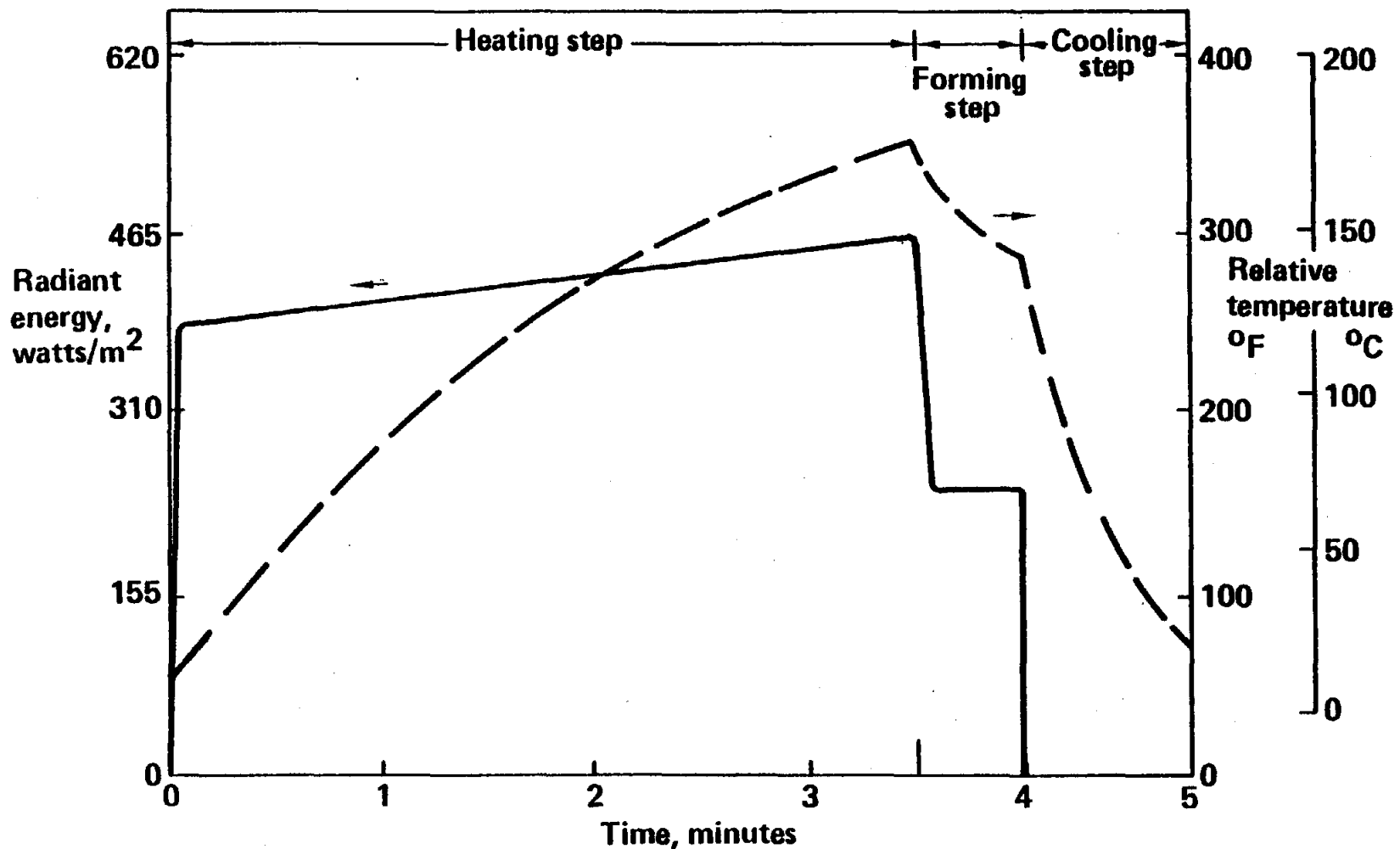


Figure 4.2-1. Typical Heat Flux & Temperature Cycle for Phase A Polyester Domes

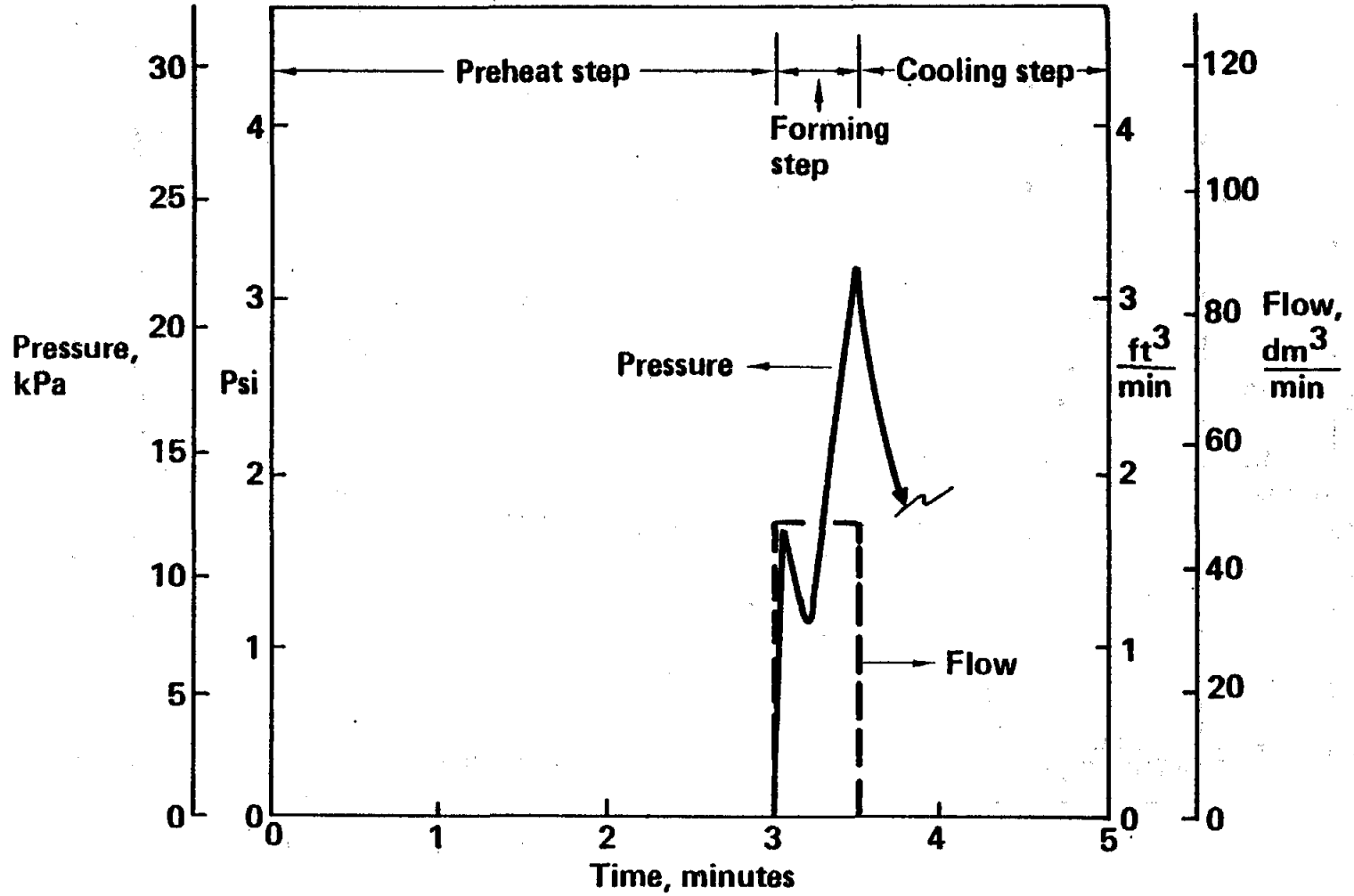


Figure 4.2-2. Typical Pressure & Flow Variation During Forming for Phase A Polyester Domes

temperature reached a predetermined level indicating that the preform was at the thermoforming temperature. At the start of the forming step the primary heaters were turned off, or removed, and the auxiliary heat lamps turned on. This resulted in the drop in radiant energy and also the reference temperature. The blowing air was turned on to a given flow rate. The pressure exerted on the film at first increased sharply and then went through a reduction before increasing again. This peak occurred at approximately the same height that the spherical curvature reaches a minimum, which is just before the dome passes through the hemispherical shape. The length of the forming step was governed by the size of the dome. When a predetermined height was reached the auxiliary heat lamps and the air flow were turned off. The dome was then allowed to cool.

5.0 PENNWALT THERMOFORMING EXPERIMENTS

5.1 INITIAL STUDY OF THERMOFORMING PARAMETERS

Kynar is a semicrystalline thermoplastic with excellent mechanical properties and resistance to weathering. It is for this reason that development of domes was undertaken with the resin. Prior to thermoforming domes, several parameters were evaluated that were believed important in determining the final properties of stretched, semi-crystalline, Kynar film. This was accomplished with an existing biaxial stretching machine. The unit was operated in a simultaneous stretching mode wherein heated flat film was stretched in two perpendicular directions at the same time. This operation simulated the phenomena experienced by the pole of a dome during a thermoforming operation.

It was first verified that the simultaneous biaxial stretching would give radial symmetry of the flat stretched film. To accomplish this, a film stretched biaxially was tested for tensile values in two perpendicular directions, each parallel to an original stretching direction, and a direction at 45° (diagonal) to the stretching directions. Table 5.1-1 summarizes the results. The films exhibited radial symmetry, hence, no statistical significance testing was required to establish the equivalence of the means of each of the tensile properties recorded. It should be noted that all tensile testing reported herein was done following the guidelines of ASTM D-882 for film.

Table 5.1-1. Tensile Testing for Radial Symmetry in Biaxially Oriented Film

<u>Sample Cut</u>	<u>20% Offset Yield</u>		<u>Break Strength</u> (Ultimate)		<u>Elongation</u>
	MPa	kpsi	MPa	kpsi	(%)
0°	100.0	14.5	211.6	30.7	155
45°	107.5	15.6	204.1	29.6	134
90°	102.0	14.8	210.9	30.6	141

Having verified that flat film stretching satisfactorily simulated dome stretching, the statistical experiment design in Table 5.1-2 was undertaken. The sixteen experiments listed were sufficient to evaluate the effects of the seven independent variables of the study. Each of the variables (columns of the Table 5.1-2) was tested at two levels, high and low. The values of each variable are listed in one table for each experiment.

Table 5.1-2 16 Run Statistical Design

Run	Resin	Mold Temp. ($^{\circ}\text{C}$)	Preform Quench	Stretch Temp. ($^{\circ}\text{C}$)	Stretch Rate (cm/sec)	Expansion Ratio	Heat Set (Minutes)
1	460	180	air	143	13.2	2 1/4	0
2	900	180	air	115	3.3	2 1/4	5
3	460	250	water	115	13.2	2 1/4	5
4	900	250	water	143	3.3	2 1/4	0
5	460	180	water	143	3.3	3 1/4	5
6	900	180	water	115	13.2	3 1/4	0
7	460	250	air	115	3.3	3 1/4	0
8	900	250	air	143	13.2	3 1/4	5
9	900	250	water	115	3.3	3 1/4	5
10	460	250	water	143	13.2	3 1/4	0
11	900	180	air	143	3.3	3 1/4	0
12	460	180	air	115	13.2	3 1/4	5
13	900	250	air	115	13.2	2 1/4	0
14	460	250	air	143	3.3	2 1/4	5
15	900	180	water	143	13.2	2 1/4	5
16	460	180	water	115	3.3	2 1/4	0

Two resin grades were studied, Kynar 900 and Kynar 460. These resins are polymerized differently and consequently have distinct thermal, rheological, and morphological properties. Because the preforms were compression molded, evaluation of mold temperature and preform quench was undertaken. From past experience it was known that molding conditions can be extrapolated to sheet extrusion conditions. The preforms were then stretched at two different temperatures using two different stretching rates. Each experiment involved stretching to a particular elongation. The values tabulated are for both perpendicular directions; hence, by 2-1/4 is meant a 2-1/4 X 2-1/4 stretch factor amplitude. Finally, subsequent to stretching, the films were either heat-set five minutes or immediately quenched.

The films from the 16 experiments were tested for percent transmission, 20% offset yield, and break strength. These tests were performed both before and after a heat treatment for 70 hours at 60°C. The change in these properties with heat aging, as well as the change in elongation to break and area change (i.e., shrinkage) were also recorded. The values for these properties are tabulated in Table 5.1-3.

To fully utilize the statistical design, a Yates' analysis was performed, and predictor equations for each of the properties was generated in terms of only those independent variables statistically significant in causing an effect. Before discussing the equations derived, certain general results are discussed. None of the original properties of the stretched film changed significantly, i.e., beyond experimental error, with heat aging. Only area shrinkage was noted and this is discussed below. The 20% offset yield, break strength, elongation to break and percent transmission were unaffected by thermal aging. In the following sections the predictor equations will be presented for each of the dependent variables.

5.1.1 Twenty Percent Offset Yield

Since the Kynar specimens in these experiments did not exhibit a true yield point in tensile properties, an offset yield was defined. In this case, a 20% offset yield was established. This is the intersection of the stress-strain curve by a line drawn from the 20% elongation point parallel to the initial portion of the curve as shown in Figure 5.1.1-1.

**Table 5.1-3. Results of the 16 Run Experimental Design
(Properties Before and After Heat Ageing 70 Hours at 60° C)**

Experiment #	20% Offset Yield				Break Strength				% Optical Transmission		% Area Shrinkage During Ageing
	Before Ageing		After Ageing		Before Ageing		After Ageing		Before Ageing	After Ageing	
	MPa	kpsi	MPa	kpsi	MPa	kpsi	MPa	kpsi			
1	68.9	10.0	73.8	10.7	108.9	15.8	109.6	15.9	81.5	80	0.14
2	93.1	13.5	95.1	13.8	176.5	25.6	169.6	24.6	55.5	55	1.93
3	81.4	11.8	76.5	11.1	141.3	20.5	128.9	18.7	87	88	1.63
4	101.4	14.7	88.9	12.9	178.6	25.9	154.4	22.4	79	88	1.42
5	85.5	12.4	86.9	12.6	146.9	21.3	146.2	21.2	91	91	2.49
6	102.0	14.8	111.0	16.1	192.4	27.9	218.6	31.7	91	90.5	2.59
7	63.4	9.2	84.1	12.2	140.0	20.3	168.9	24.5	80	77	0
8	92.4	13.4	100.7	14.6	138.6	20.1	142.7	20.7	70.5	71	0.65
9	168.9	24.5	97.2	14.1	204.8	29.7	214.4	31.1	91.5	90	3.08
10	78.6	11.4	78.6	11.4	146.9	21.3	134.4	19.5	91	90	1.45
11	107.6	15.6	104.8	15.2	203.4	29.5	200.6	29.1	66.5	75	2.55
12	82.7	12.0	73.8	10.7	151.0	21.9	135.1	19.6	69.5	73	1.40
13	114.5	16.6	103.4	15.0	197.2	28.6	167.5	24.3	57	56	2.76
14	73.1	10.6	74.5	10.8	116.5	16.9	118.6	17.2	83.5	80	0.32
15	75.2	10.9	71.7	10.4	144.1	20.9	122.7	17.8	82.5	76	1.03
16	77.2	11.2	79.3	11.5	156.5	22.7	152.4	22.1	89.5	86	2.77

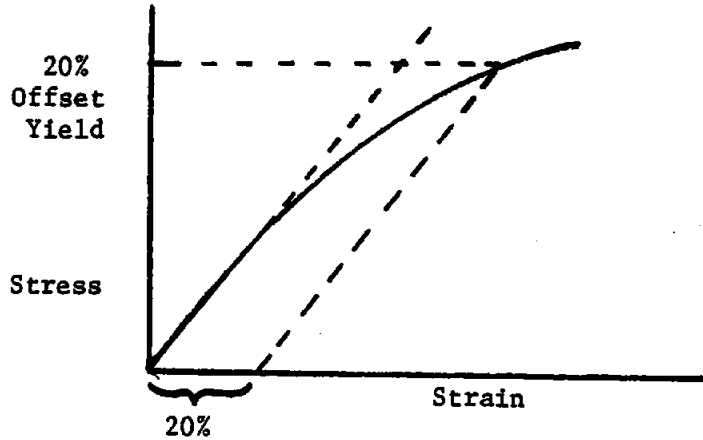


Figure 5.1.1-1. Schematic of the Definition of 20% Offset Yield

From the sixteen run study the predictor equation for the 20% offset yield is:

$$T_Y^{20\%} = 91.6 \text{ MPa} + 15.2 (\text{Resin}) + 6.0 (\text{Exp. Ratio}) - 6.9 (\text{Stretch Temp.})$$

The other four variables were insignificant in changing the yield. To use the equation, the high level of each variable is designated at +1 while the low level is -1. Hence, for the high level of resin (Kynar 900) 15.2 MPa is added to the 91.6, and for the one low level of resin (Kynar 460), 15.2 MPa is subtracted. Similarly, for a combination of the high expansion ratio and the low stretching temperature an additional 12.9 MPa is added.

Using the high expansion ratio, the offset yield is far greater with Kynar 460 than the required value. Figure 5.1.1-2 is a graph of the predictor equation for 20% offset yield as a function of stretch temperature for Kynar 460 stretched 3-1/4 times. The dotted line is the minimum value required.

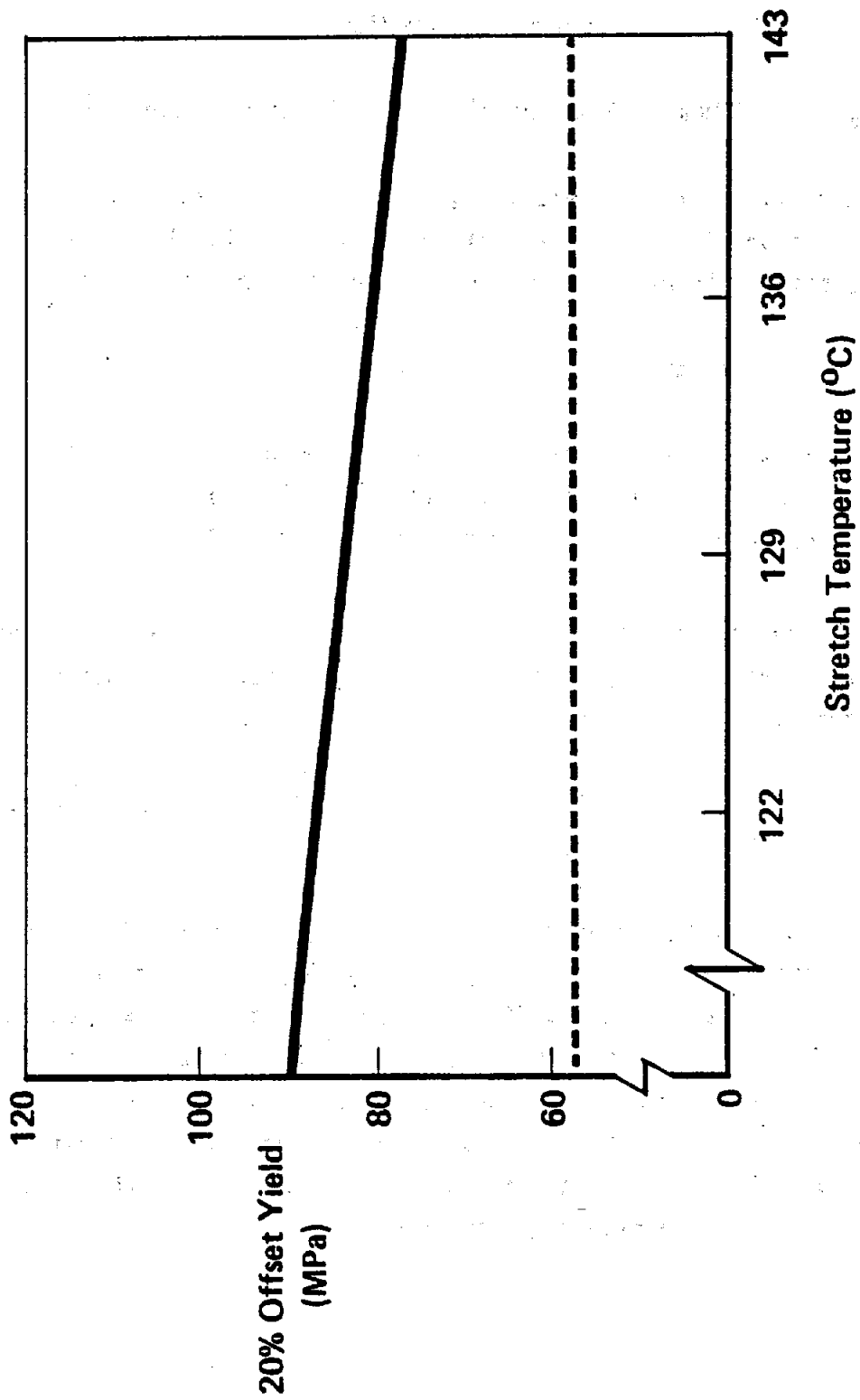


Figure 5.1.1-2. 20% Offset Yield vs. Stretching Temperature for Kynar 460

5.1.2 Break Strength

The stress recorded when the film breaks is also a function of its preparation parameters. For this property, the predictor is:

$$T_B = 158.9 \text{ MPa} + 20.5 (\text{Resin}) - 11.0 (\text{Stretch Temperature})$$

The other five variables were insignificant. The predictions for Kynar 460 are shown in Figure 5.1.2-1. The minimum break strength allowable is 94.8 MPa (13,750 psi). Clearly there was no problem in achieving this.

5.1.3 Transmission After Heat Aging

The optical transmission test performed at Pennwalt was carried out at 550 nm wavelength using an integrating sphere with a $1/2^\circ$ acceptance angle. It was shown to correlate well with the test performed at Boeing.

Since the optical transmission is not significantly altered with heat aging, and optimizing this property is desired, only its predictor equation after heat aging is reported. The equation is:

$$T = 79.2 - 3.97 (\text{Resin}) + 3.03 (\text{Exp. Ratio}) + 2.2 (\text{Str. Temp.}) \\ - 8.28 (\text{Preform Quench})$$

Evidently quenching the preform from the melt into water is advantageous. This process limits the size of the crystals so they are not efficient scatterers of light in the final stretched film. Kynar 460 shows a marked advantage. A 4% addition to the transmission is achievable using this resin. It is for this reason that Kynar 460 is the resin of choice for solar application. Its molecular weight and molecular distribution obviously cause changes in its crystallization that are beneficial. Using the predictor equation, Figure 5.1.3-1 shows that excellent transmissions can be expected from domes.

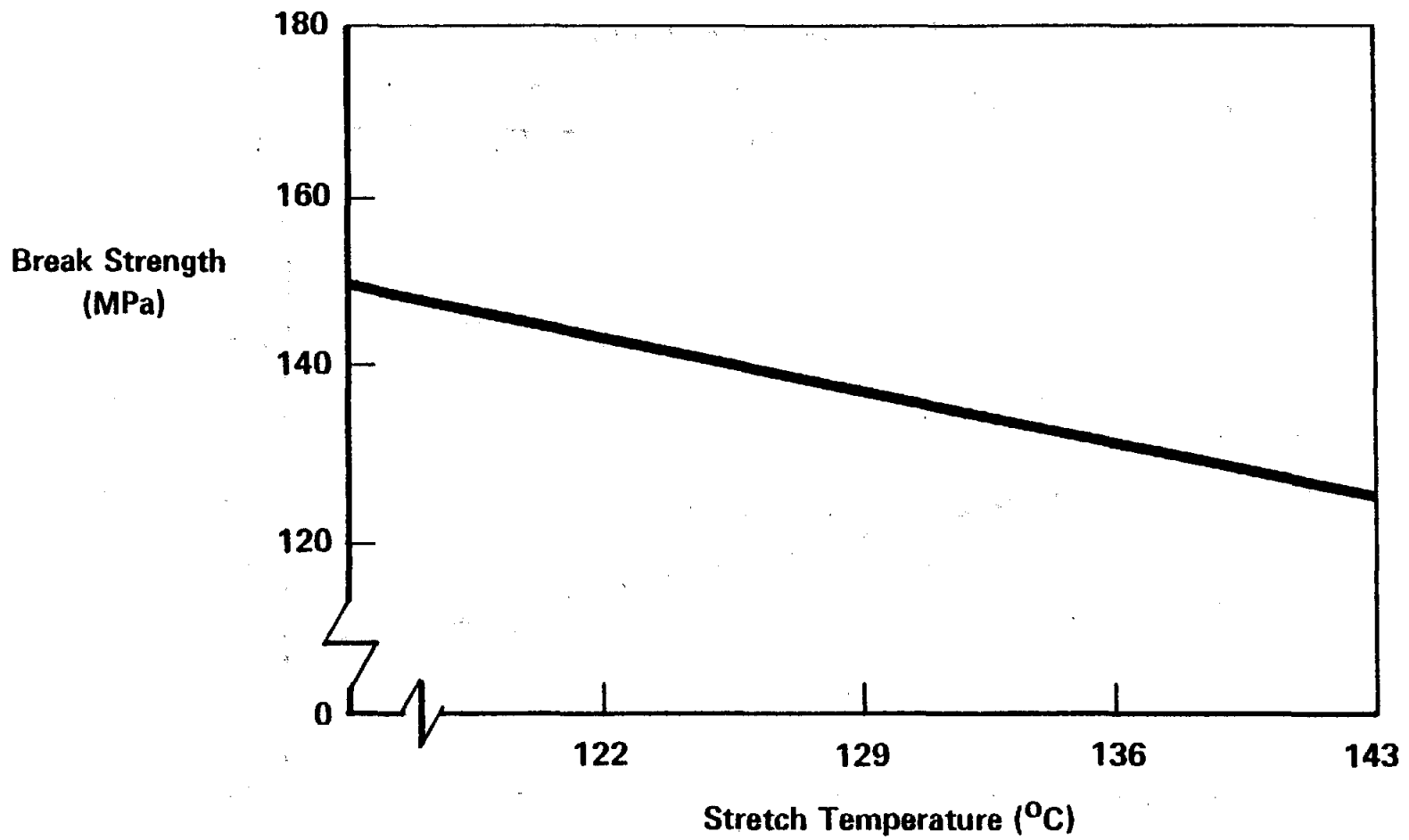


Figure 5.1.2-1. Break Strength vs. Stretch Temperature for Kynar 460

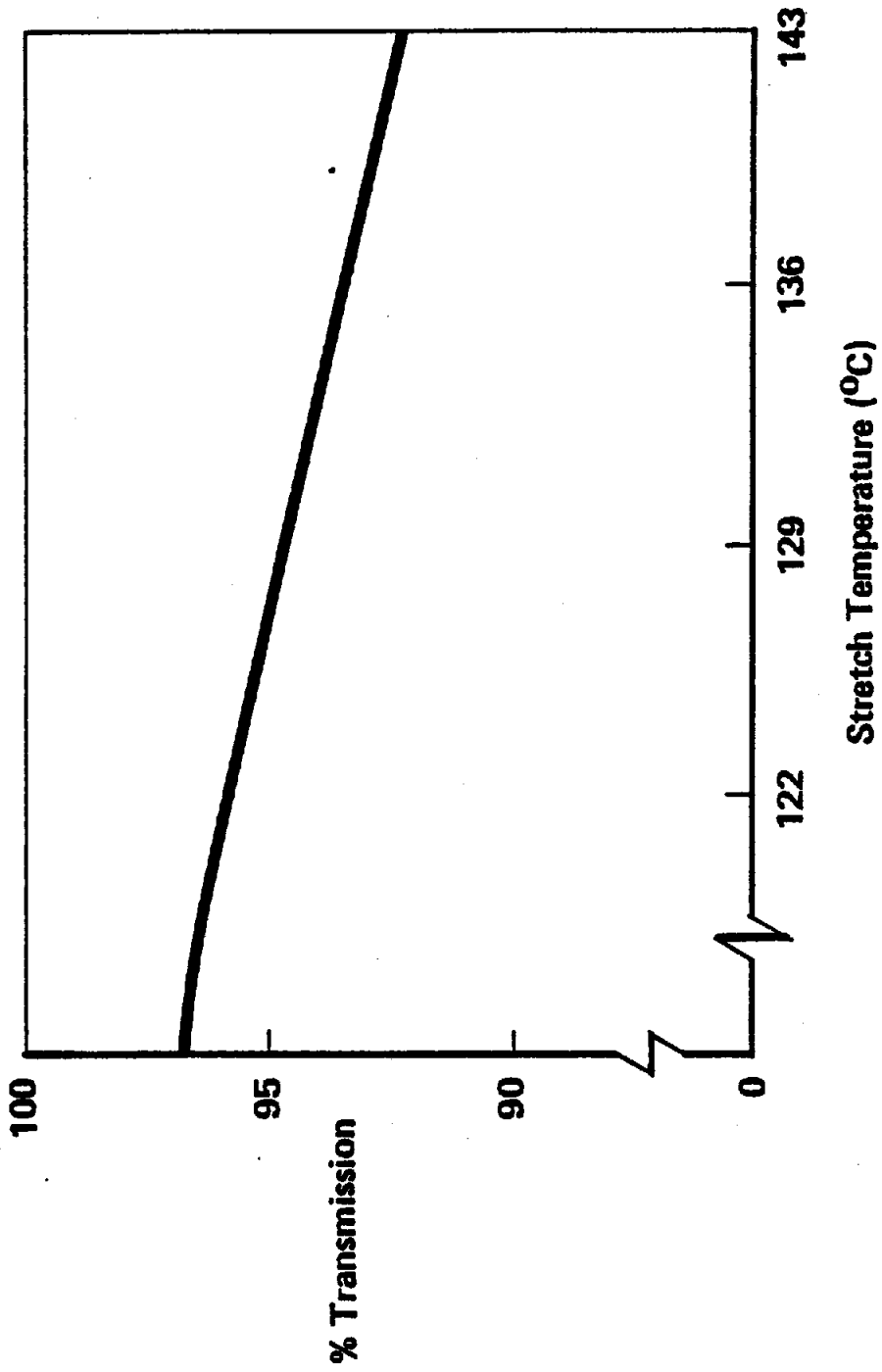


Figure 5.1.3-1. % Transmission vs. Stretching Temperature for Kynar 460

5.1.4 Area Change After Heat Aging

The area change is reported as shrinkage, that is, a positive value corresponds to an area decrease. The prediction is:

$$\Delta A\% = 1.62 + 0.38 (\text{Resin}) - 0.4 (\text{Str. Temp.}) - 0.44 (\text{Quench})$$

Area change is given in Figure 5.1.4-1 as a function of stretching temperature. As shrinkage cannot be totally avoided, it can at least be minimized and tolerance designed into the final product.

5.2 PHASE A KYNAR THERMOFORMING RESULTS (PENNWALT)

5.2.1 Process Experiments

In Phase A twenty-five compression molded preforms of Kynar 460 were prepared for thermoforming using the desirable conditions as determined above. These together with Kynar 460 sheet extruded at Pennwalt were thermoformed in the Phase A facility at Boeing. The compression molded preforms were 0.76 mm (30 mils) thick and the sheet was 1.52 mm (60 mils). It was intended in this part of the work to gain practical information on thermoforming Kynar domes.

Approximately 24 domes 35.5 cm (14 in) in diameter were formed both from the compression molded preforms and extruded sheet. Table 5.2.1-1 is a summary of the thermoforming conditions. The most difficult variable to assess was preheat time under infra-red lamps. Kynar resin being a fluoropolymer does not absorb as strongly in the 3500 nm range as hydrocarbon polymers do. In fact, it absorbs very strongly at 7000 nm and above. Hence, preheat time was important. It was necessary to preheat for the minimum time that would allow blowing at the highest pressures attainable. The combination of low temperature and high pressure (or stretch rate) was known from the earlier study to give the best mechanical and optical properties. This fact was confirmed visually during the thermoforming operation. Several of the domes were clear while others had a haze. The haze is attributable to an excessive temperature during thermoforming.

Table 5.2.1-2 is a summary of tensile properties for a dome blown at low internal pressure (#11) and one blown at high internal pressure (#17). Samples were cut from

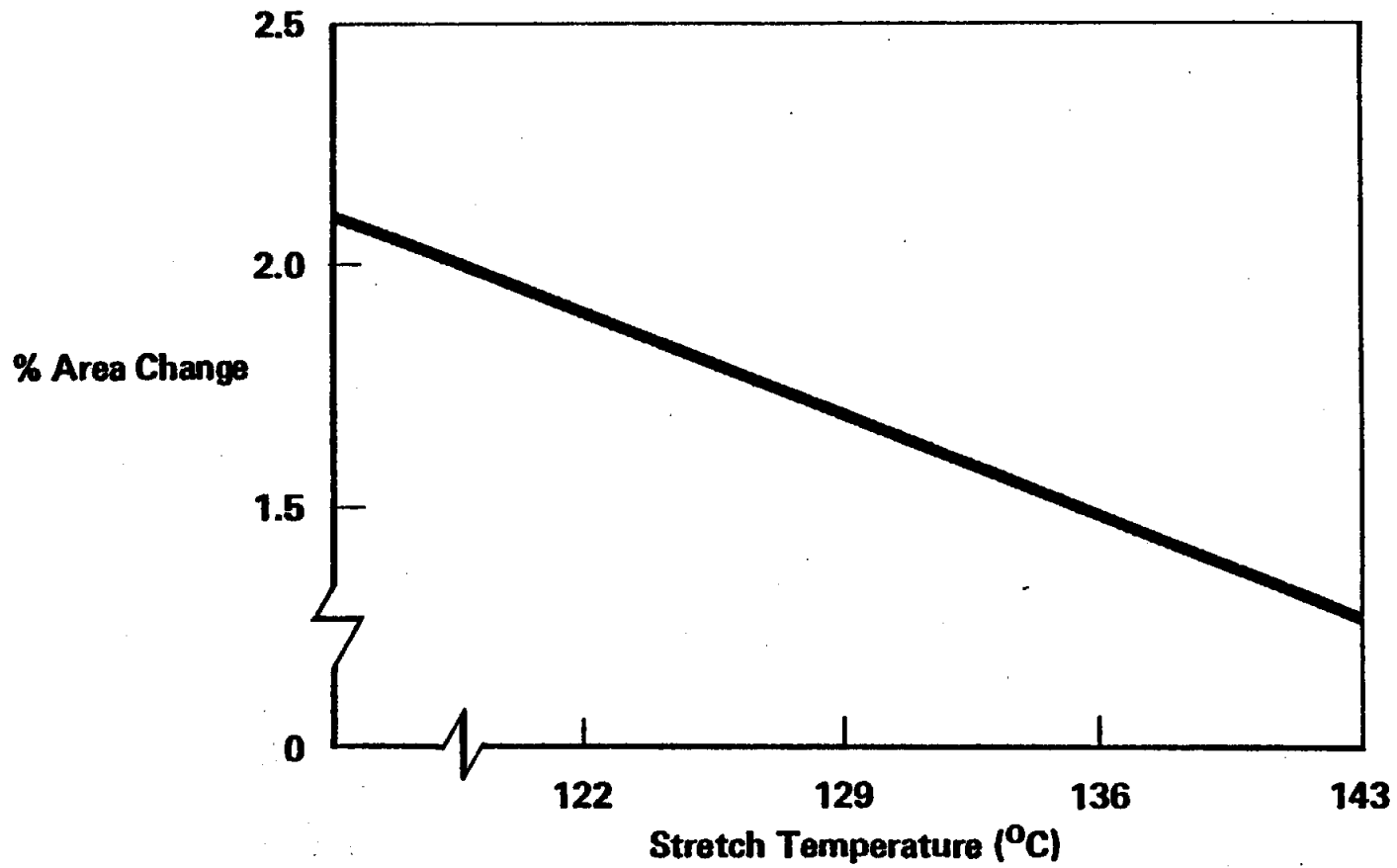


Figure 5.1.4-1. % Area Change vs. Stretching Temperature for Kynar 460

Table 5.2.1-1. Summary of Thermoformed Runs in Boeing Phase A Facility

Bubble #	6	9	11	12	13	17	18	19
Preform	C. M.*	C. M.	C. M.	C. M.	C. M.	Ex.**	Ex.	Ex.
Preheat								
Time	5 min	4 1/2 min	4 1/2 min	4 min	3 1/2 min	5 min	6 min	5 min
Lamp Intensity								
Bottom	100%	100%	100%	100%	100%	100%	100%	100%
Top	100%	100%	100%	100%	100%	100%	100%	100%
Center Top	100%	100%	100%	100%	100%	100%	100%	100%
Blowing Operation								
Lamp Intensity								
Bottom	100%	100%	100%	100%	100%	100%	Off	Off
Top	100%	100%	100%	100%	100%	100%	Off	Off
Center Top	Off	Off	Off	Off	Off	Off	Off	Off
Set Pressure (kPa)	34.5	29.6	34.5	32.7	51.7	68.9	62.0	68.9
Maximum Recorded								
Pressure (kPa)	20.7	29.6	11.7	34.5	37.2	68.2	37.9	48.6

* C. M. = compression molded

**Ex. = extruded

31

Table 5.2.1-2 Tensile Data of Selected Domes Formed in Boeing Phase A Facility

<u>Dome #11</u>	<u>20% Offset Yield</u>		<u>Break Strength</u>		<u>Elongation to Break</u>
	MPa	kpsi	MPa	kpsi	%
PL	88.2	12.8	155.7	22.6	112
BL	110.2	16.0	154.3	22.4	74
E	68.2	9.9	105.4	15.3	153
<u>Dome #17</u>					
PL	116.4	16.9	194.3	28.2	82
BL	117.1	17.0	188.8	27.4	92
E	73.7	10.7	130.9	19.0	146

3 positions on the dome. The "PL" samples were taken at the top of the dome and were tested in a longitudinal direction (vertical). The "BL" samples were taken at the side of the dome and also tested longitudinally (vertical). The "E" samples were taken near the base of the dome and tested horizontally. All samples were tested as per ASTM D-882. The direction of testing coincides with the long dimension of the strips.

The superior tensile properties of dome #17 are probably the result of lower film temperature during blowing, as indicated by the higher required blowing pressure. The comparatively large elongations-to-break of the equatorial samples indicate incomplete stretching in this direction. This in turn is due to a lack of heating in these regions.

The next step in the development of thermoformed domes was to prepare domes of 61 cm (24 in) diameter at Pennwalt. As there was insufficient time to have an infra-red oven designed and built in Phase A, a circulating hot air oven was prepared for this service. A 689 kPa (100 psi) compressed air line was regulated by a high flow volume pressure regulator. The temperature profile in the oven was non-uniform.

This was determined using an IRCON infra-red pyrometer, which indicated as much as 26°C differential between walls in the oven and an 18°C difference between oven setting and the coldest wall. This problem could not be alleviated. However, 48 cm preforms were cut from extruded sheet and a program was begun to prepare the best domes possible in spite of this shortcoming.

In general, the equatorial region of the domes did not stretch well. Also, the hot walls of the oven emitted thermal energy to the growing dome while the dome emitted to the cold walls. Hence, non-uniformity of shape often resulted although it was minimized. Again, thickness profile and shape measurements are not indicative of the potential. By proper empirical adjustment of temperature and pressure, domes of excellent mechanical and optical properties were prepared and delivered to Boeing personnel for desert exposure. Rather than present the evolutionary work that resulted in these sample domes, only the data recorded for the higher quality domes are given. Table 5.2.1-3 is a summary of the mechanical and optical properties of these domes. The coding described earlier for tensile testing of samples is used here. In general, the better tensile values were obtained on domes blown

Table 5.2.1-3. Summary of Data on Kynar 460, 61 cm (24 in) Domes

Dome #	1	9	11	12	14
20% Offset Yield (MPa)					
PL	109.3	112.1	121.3	130.8	151.7
BL	110.0	N. T.	N. T.		114.7
E	70.5	N. T.	N. T.		96.2
Break Strength (MPa)					
PL	170.0	179.9	188.7	211.7	211.3
BL	158.2	N. T.	N. T.		196.5
E	138.7	N. T.	N. T.		162.0
Elongation to Break (%)					
PL	106	106	95	96	82
BL	94	N. T.	N. T.		104
E	133	N. T.	N. T.		124
Transmission (%)					
@ 550 nm	94	91	92.5	92.5	92

more quickly. All were blown at an oven setting of 178⁰C except #14 which was blown at 175⁰C. This number, because of the poor temperature profile of the oven, unfortunately does not reflect the sheet temperature (if the sheet had reached this temperature, it would have melted).

5.2.2 Environmental Test Domes

The Kynar domes being tested by Boeing were thermoformed by Pennwalt. The first dome listed in Table 5.2.2-1, the "Forming Example" dome, was fabricated in the Boeing facility with a diameter of approximately 38 cm (15 in). The others were larger, approximately 61 cm (24 in) in diameter, and formed using the modified hot air oven. The mechanical properties are given in Table 5.2.2-1 and the transmittance values in Table 7.2-6. These values will be used for subsequent comparison of data from desert exposure domes.

5.3 PHASE B THERMOFORMING FACILITY (PENNWALT)

To thermoform 1.2 m (4 ft) diameter domes in Phase B, a 1.83m (6 ft) cubical chamber was utilized. It was constructed of steel with Maronite insulation on the inner walls. Heat to the 86 cm (34 in) diameter preform was provided by radiation from infrared sources located at three levels within the chamber. Reference to Figure 5.3-1 will facilitate description of the details. The top heaters, in the ceiling, are slow-response planar, infrared emitters. The emitting surface is 1.5 m X 1.5 m square with the center 0.9 m X 0.9 m capable of being lowered closer to the preform (see #2 Figure 5.3-1). The temperature of the entire ceiling panel was controlled utilizing a thermocouple imbedded in one of the heater units.

The infrared heaters located in the center of the oven and at the bottom, numbered 3 and 4 respectively, were arranged in a ring encircling the dome. They were quartz-jacketed tubular emitters. Unlike the ceiling panel, they were fast response heaters capable of quicker temperature changes on demand. The temperatures of the center and bottom ring were independently controlled.

Dome	Position	Direction	Yield stress		Ultimate stress		Elongation %	Yield strength	
			MPa	kpsi	MPa	kpsi		kN/m	lbs/in
One piece (forming example)	Top	Vertical	91.7	13.3	171.7	24.9	76	6.6	37.7
		Horizontal	88.2	12.8	160.6	23.3	78	6.3	36.1
	Side	Vertical	89.6	13.0	153.8	22.3	82	7.0	40.0
		Horizontal	75.2	10.9	132.4	19.2	95	6.7	38.4
	Bottom	Vertical	88.2	12.8	150.3	21.8	121	12.5	71.3
		Horizontal	49.0	7.1	81.4	11.8	228	8.3	47.6
One piece (test)	Top	Vertical	94.5	13.7	153.1	22.2	78	7.7	43.9
		Horizontal	97.2	14.1	162.7	23.6	79	7.4	42.4
	Side	Vertical	80.0	11.6	138.6	20.1	101	9.0	51.2
		Horizontal	79.3	11.5	137.9	20.0	117	8.7	49.7
	Bottom	Vertical	81.4	11.8	137.2	19.9	137	15.2	86.9
		Horizontal	62.0	9.0	104.8	15.2	199	11.3	64.7
One piece (environmental test)	Top	Vertical	98.6	14.3	159.3	23.1	91	9.1	51.8
		Horizontal	98.6	14.3	162.7	23.6	82	8.9	50.6
	Side	Vertical	94.5	13.7	168.2	24.4	102	11.7	66.7
		Horizontal	74.5	10.8	127.6	18.5	148	10.1	57.8
	Bottom	Vertical	98.6	14.3	156.5	22.7	127	19.8	113
		Horizontal	52.4	7.6	88.2	12.8	287	13.2	75.2

Table 5.2.2-1. Kynar Domes—Mechanical Properties

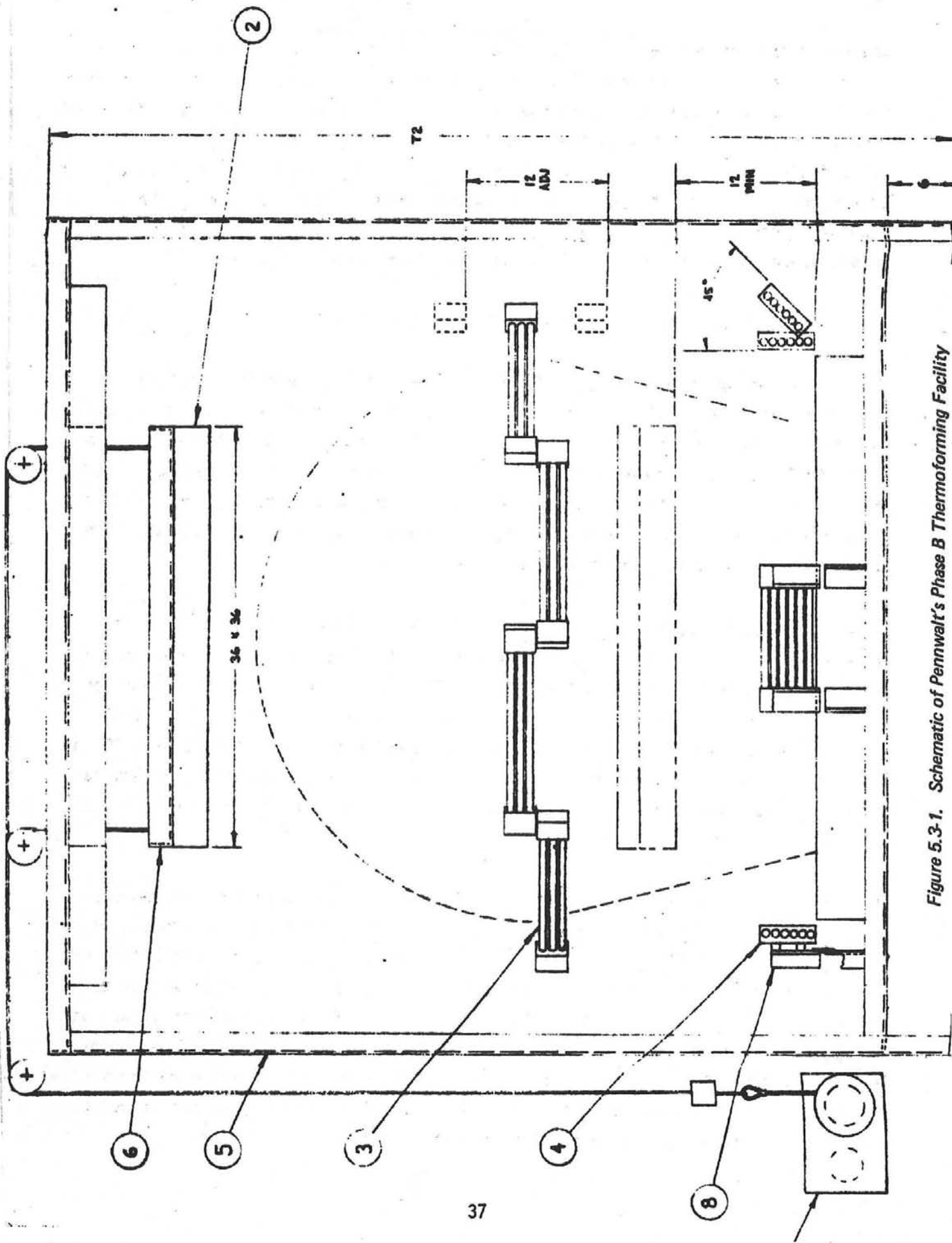


Figure 5.3-1. Schematic of Pennwalt's Phase B Thermoforming Facility

The Kynar preform was held on a base shown in Figure 5.3-2 with an annular ring and clamps. Air was introduced at the bottom of the base through a diffuser. The air supply was a compressor supplying 689 kPa (100 psi) pressure to a Moore Model 42H30 pressure regulator which adjustably limits the downstream pressure to values between 6.9 and 207 kPa. An open-end air flow of 3.54 m³/min (125 scfm) is deliverable from this regulator. The internal pressure of the dome was monitored during thermoforming by an Ametek Model #58G 0015BN2 pressure transducer with output to an oscillographic recorder. Figure 5.3-3 is a picture of the entire facility.

5.4 PHASE B KYNAR THERMOFORMING RESULTS (PENNWALT)

For the scaled-up domes required in Phase B, the facility described in Section 5.3 was used. From the initial studies and thermoforming runs of Phase A it was expected that good quality domes would result from quick blowing at temperatures between 140-150°C. Therefore as an initial task the infrared heaters had to be characterized. That is, the Athena controllers settings and therefore the infrared heater emissions had to be adjusted so as to efficiently heat the Kynar which absorbs most strongly at 7000 nm wavelength and above.

The actual heating behavior of the Kynar preform is shown in Figure 5.4-1 for several ceiling, infrared heater temperatures. The temperatures were monitored by a thermocouple sandwiched between two 1.52 mm Kynar preforms. The Athena controller was set to a temperature and measurements began when the ceiling panel equilibrium was reached. For this series of experiments the center 90 cm X 90 cm ceiling section was lowered to 30 cm from the Kynar after it had reached temperature. As expected the Kynar responds best at the higher emitter temperatures, and levels out at long times.

Thermoforming experiments were performed with the oven walls at ambient temperature at the beginning of the heat-up. Figure 5.4-2 is a plot of the profile of temperature across the diameter of the preform for a ceiling panel temperature of 260°C. Thermocouple #4 is the center with all the others equally spaced out to the edge. The variation in temperature across the preform shown in the figure was unacceptably large, resulting in deformation of the center of the preform at the expense of the outer perimeter. The ring of bottom tubular heaters were ineffective in alleviating this profile. For future work these lights could be put to better use if they were directed towards the perimeter region of the preform.

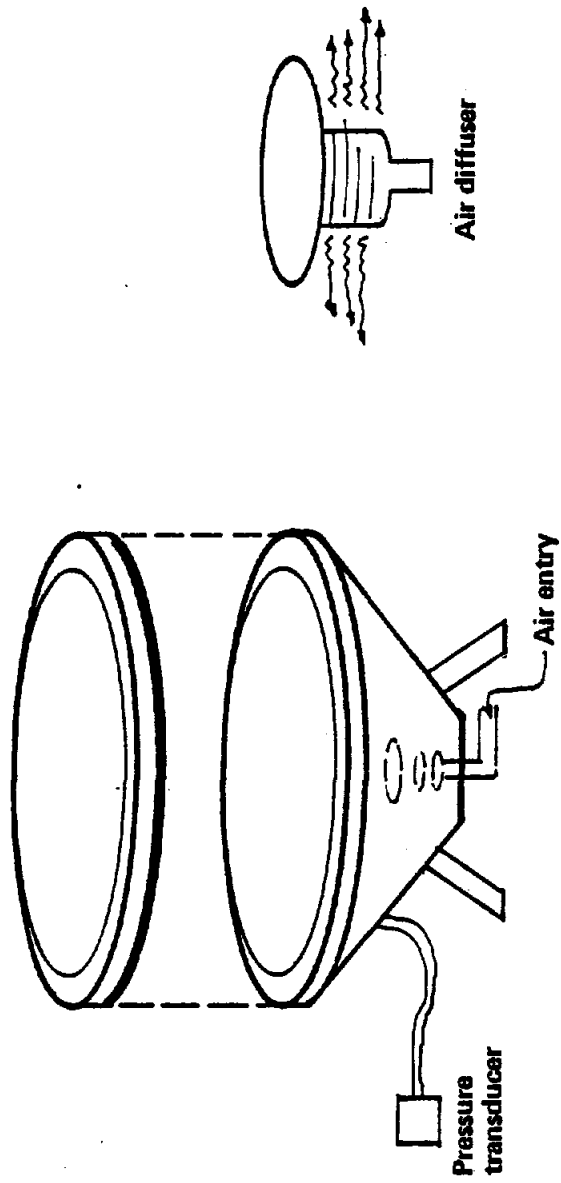


Figure 5.3.2 Preform Holder and Air Diffuser

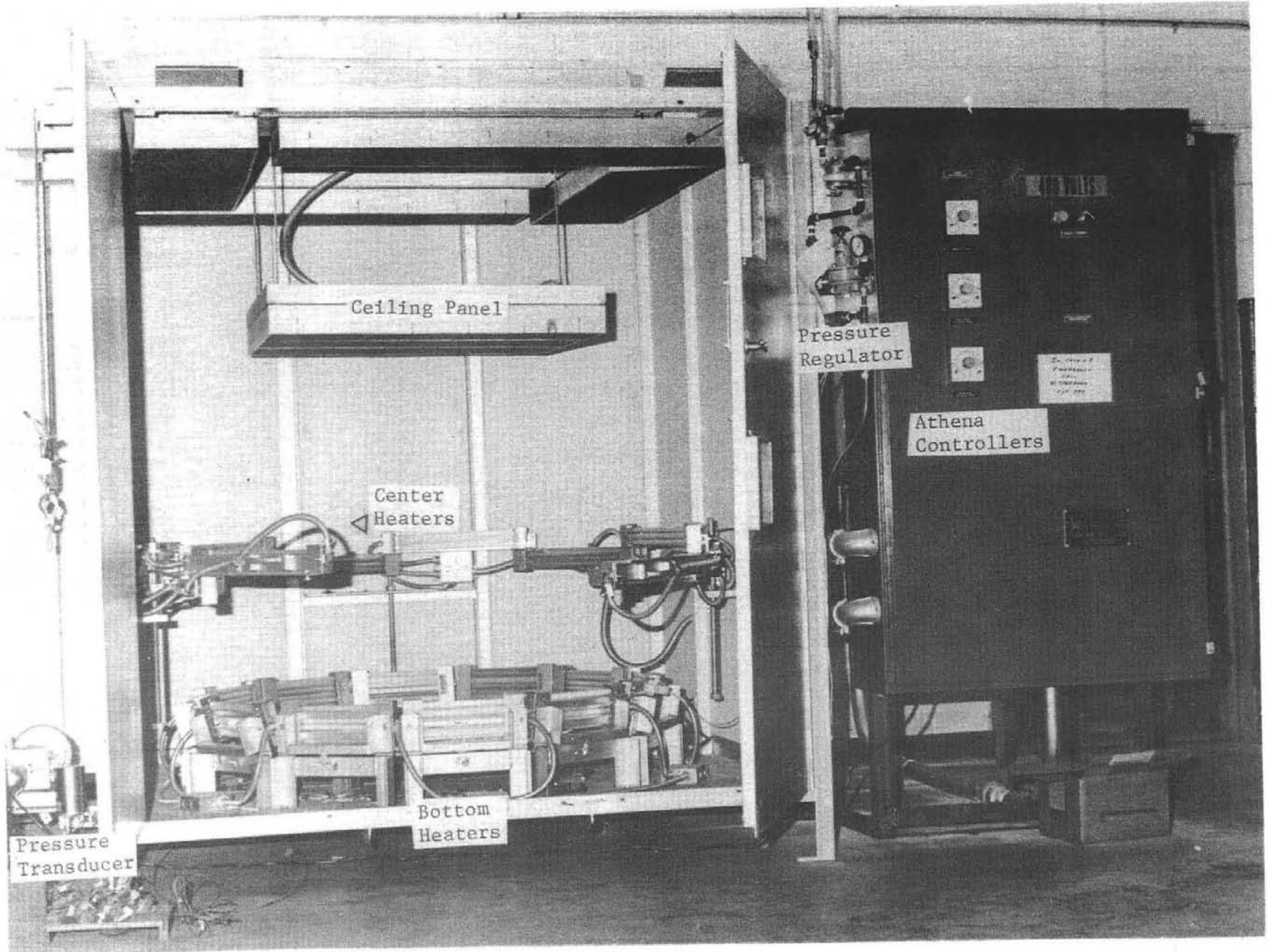


Figure 5.3-3. Pennwalt's Thermoforming Facility - Phase B

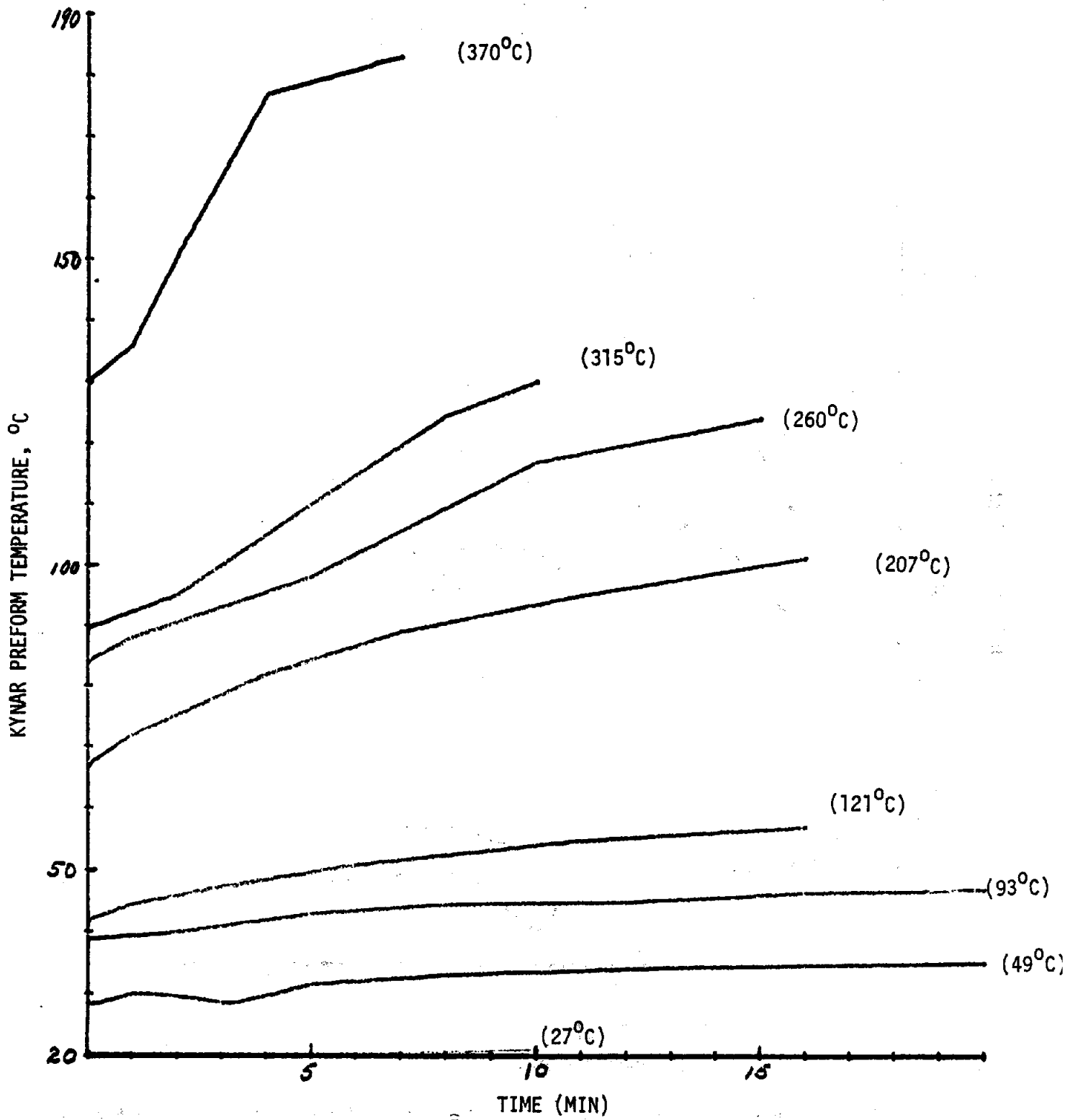


Figure 5.4-1. Effect of Infrared Heater Temperature on Kynar Heating Characteristics

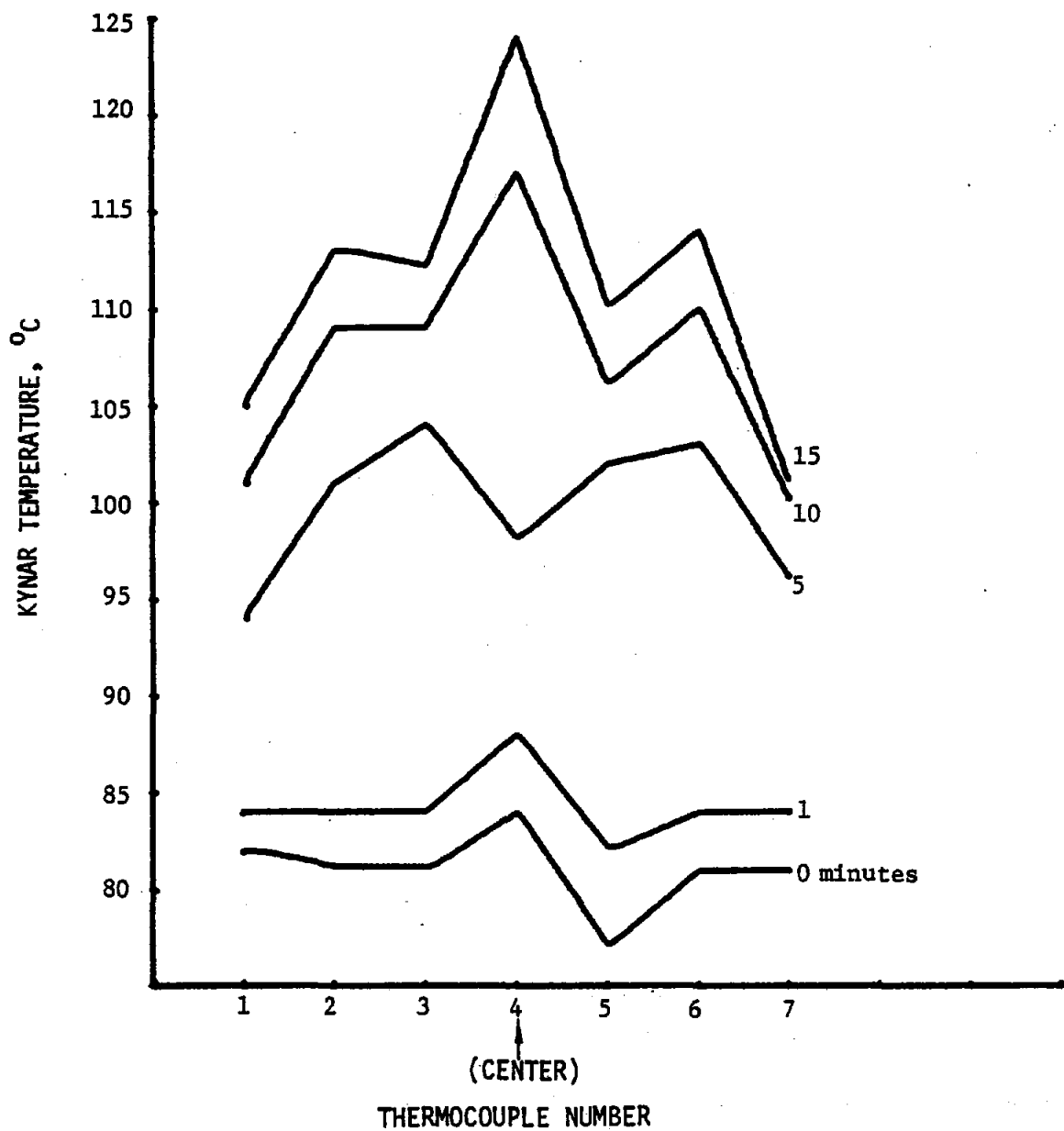


Figure 5.4-2. Temperature Profile Across Diameter of the Preform (Infrared Heater Setting = 260° C)

Alternately, the ceiling panel should either have a temperature profile increasing radially from the center to edge, or be much larger than the preform.

To alleviate the temperature profile in the present effort, a circular Kynar sheet 25.4 cm in diameter and 0.76 mm thick was used to shield the center of the preform during heating. In addition the center panel of the ceiling radiant heater was raised to approximately 1.5 m from the preform. This was done to provide more uniform heating over the preform.

In addition to preform temperature non-uniformity, difficulties were also encountered with the air supply used for forming domes. In the initial air supply apparatus, insufficient volumetric air flow was available to form domes at desired growth rates. A larger pressure regulator, described earlier, was incorporated to alleviate this problem.

To date, no satisfactory Kynar domes have been thermoformed with the Phase B Pennwalt facility. Domes produced were generally non-spherical in shape, or, because of air supply limitations in early experiments, cooled before they could be properly formed.

5.5 WEATHEROMETER TESTS

Samples for weatherometer tests were cut from 61 cm (24 in) diameter Kynar domes prepared in Phase A. Specimen locations included the pole (PL), longitudinally from the side (BL) and latitudinally from the side (E). Tedlar film* was also included in the test for reference purposes. All samples were 1/2 in. wide, conforming to specifications in ASTM D 882 for tensile testing of film. Tensile and optical properties of one half the samples were measured and recorded. The other half were subjected to accelerated weathering in an Atlas Dew Cycle Weatherometer operating without filters for the carbon arc. This test is recognized as the most severe accelerated weathering test.

Weathering of film is accomplished by repetitive two-hour cycles. During the first hour films are subjected to light from arcing carbon electrodes. The light

* DuPont polyvinyl fluoride, 400 SG(EXP)TR, co-polished with Mylar (DuPont 200 X M648A)

is rich in UV especially below 300 nm. Temperature of the black panel inside the weatherometer was $63 \pm 2.5^{\circ}\text{C}$ ($145 \pm 5^{\circ}\text{F}$), air temperature was $44.5\text{-}49^{\circ}\text{C}$ ($112\text{-}120^{\circ}\text{F}$) and the relative humidity was 50%. The second hour was a dark cycle wherein the relative humidity was maintained greater than 95%, and air temperature was dropped to $26.5\text{-}31^{\circ}\text{C}$ ($80\text{-}88^{\circ}\text{F}$).

After 558.8 hours of continuous exposure the samples were removed and tested. It has been the experience of personnel in the Kynar Coating Department at Pennwalt that 100 cycles of the carbon arc weatherometer has correlated with 3-5 years outdoor exposure. On this basis, the exposure approximates 16-28 years of outdoor weathering. It is apparent from Tables 5.5-1 and 5.5-2 that Kynar withstood the exposure quite successfully. The Tedlar became brittle and very hazy. Figures 5.5-1, 5.5-2 and 5.5-3 are semilog plots of the normalized 20% offset yield; break tensile and ultimate elongation for Tedlar, and the pole samples from each Kynar dome. Normalized values are calculated by dividing the tensile property after exposure, by the control's value. Figure 5.5-4 is a semilog plot of the optical transmission change after weathering. These figures summarize visually the changes reported in the tables.

Table 5.5-1. Tensile Testing of Kynar–Tedlar (Control and After 558.8 Hours of Weatherometer Exposure)

<u>Sample</u>	<u>20% Offset Yield</u>		<u>Break Tensile</u>		<u>Elongation to Break</u>
	MPa	kpsi	MPa	kpsi	%
<u>TEDLAR</u>					
Control	34.5	5.0	61.4	8.9	372
Exposed	-	-	60.7	8.8	23
<u>KYNAR</u>					
<u>Dome 6</u>					
PL	111.0	16.1	189.5	27.5	144
Exposed PL	127.5	18.5	182.7	26.5	105
E	77.2	11.2	137.2	19.9	197
Exposed E	72.4	10.5	104.8	15.2	177
BL	93.8	13.6	159.4	23.1	142
Exposed BL	113.7	16.5	171.1	24.8	133
<u>Dome 7</u>					
PL	88.2	12.8	142.8	20.7	154
Exposed PL	104.8	15.2	137.3	19.9	124
E	80.7	11.7	151.8	22.0	193
Exposed E	77.9	11.3	129.0	18.7	176
BL	84.8	12.3	145.6	21.1	173
Exposed BL	86.2	12.5	134.5	19.5	136
<u>Dome 15</u>					
PL	91.7	13.3	155.9	22.6	145
Exposed PL	104.8	15.2	143.5	20.8	130
E	97.9	14.2	140.7	20.4	128
Exposed E	95.8	13.9	132.5	19.2	106
BL	83.4	12.1	147.6	21.4	115
Exposed BL	102.0	14.8	137.3	19.9	104

Table 5.5-2. Transmission Before and After Accelerated Weathering

Sample	Tedlar	KYNAR					
		#6PL	#6E	#7PL	#7E	#15PL	#15E
% Transmission							
Before Exp.	89.5	90.0	88.5	88.5	88	89.5	89.0
After Exp.	45	86.5	86.0	87.5	84	82	85.5

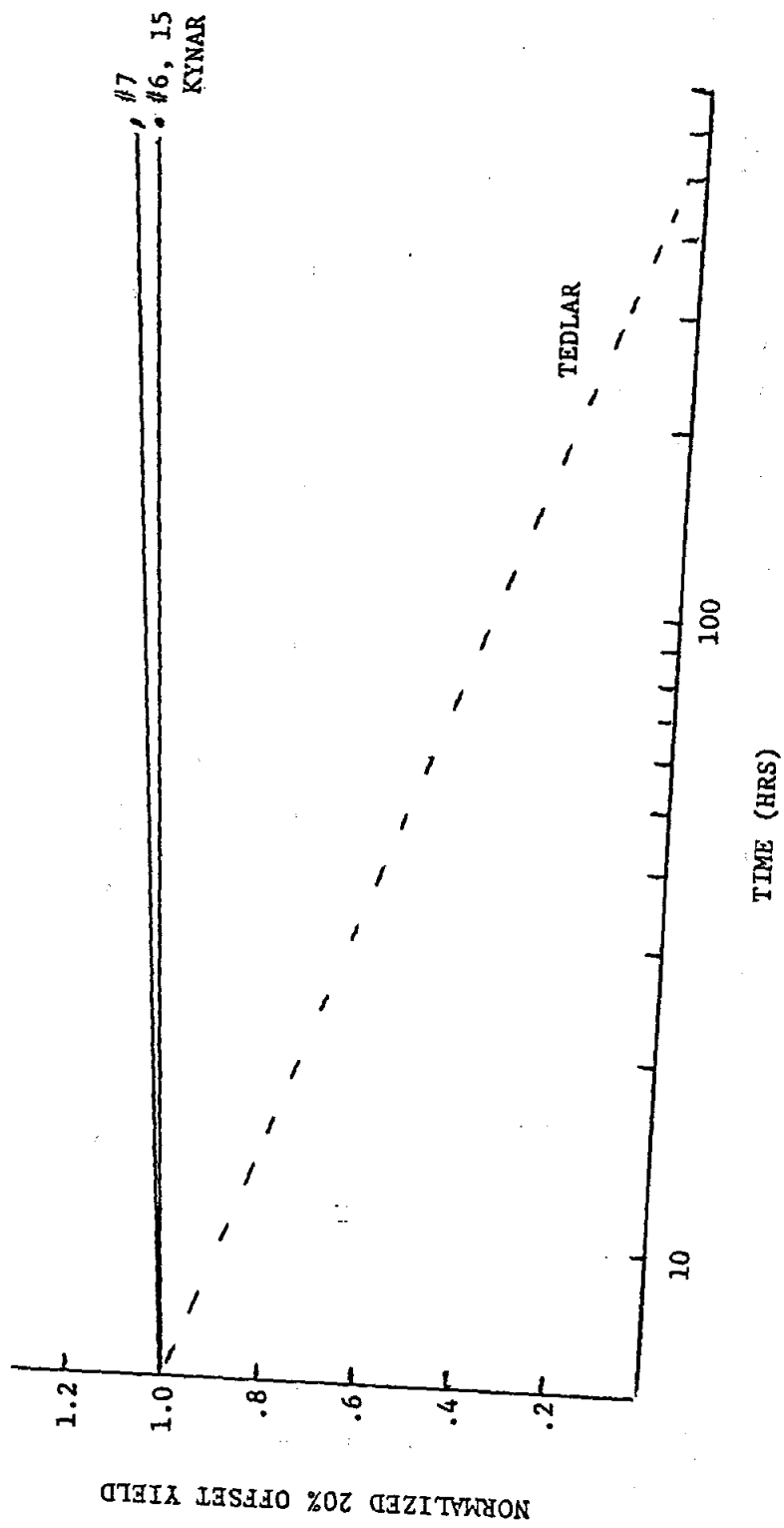


Figure 5.5-1. Normalized 20% Offset Yield vs. Hours in the Weatherometer

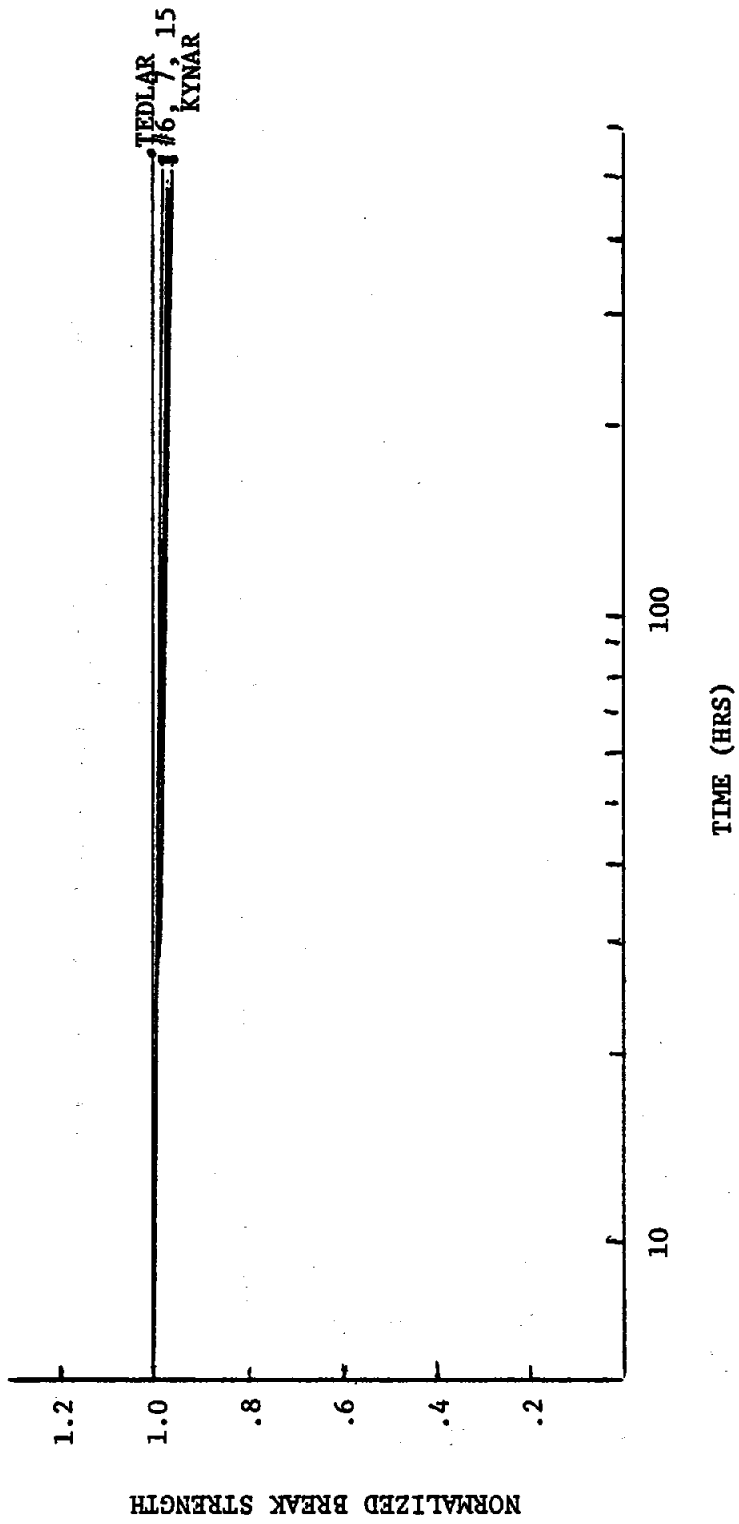


Figure 5.5-2. Normalized Break Strength vs. Hours in the Weatherometer

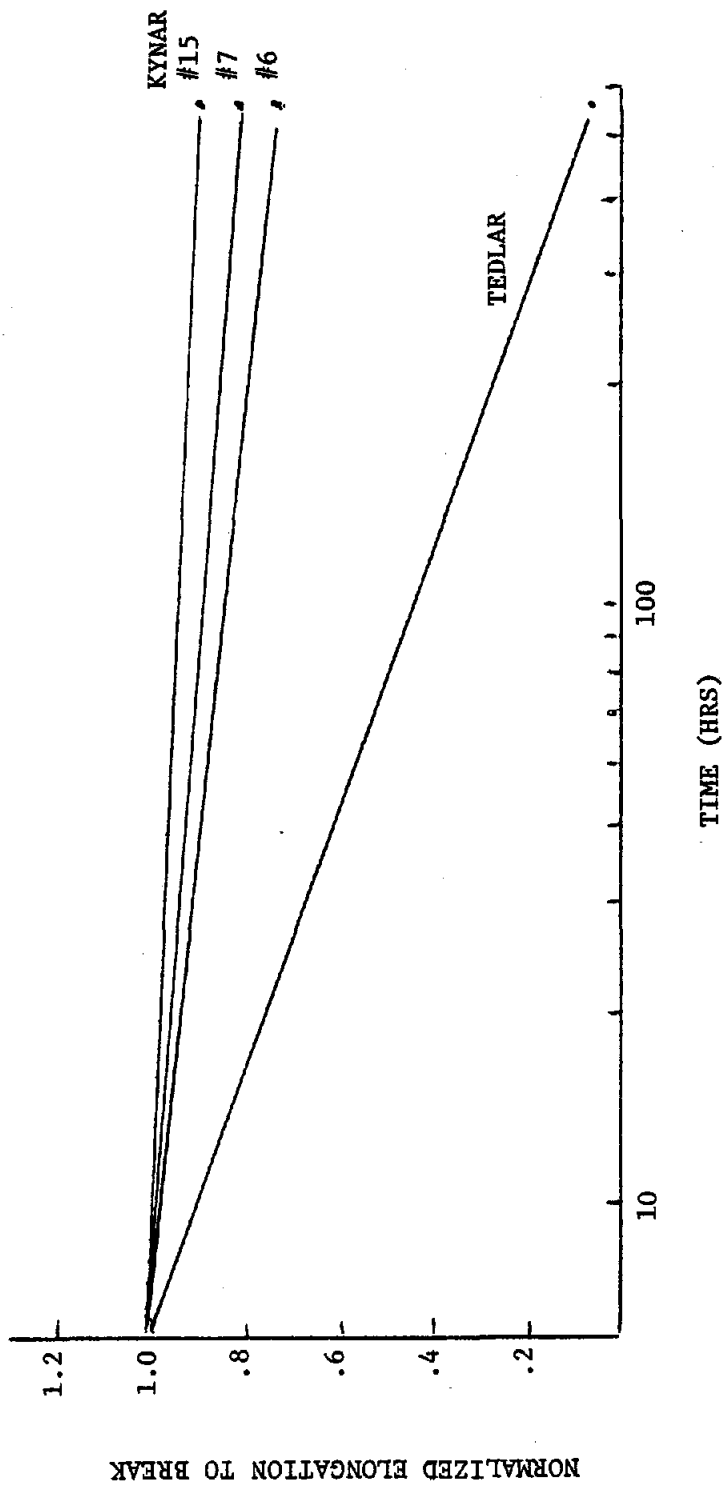


Figure 5.5-3 Normalized Elongations vs. Hours in the Weatherometer

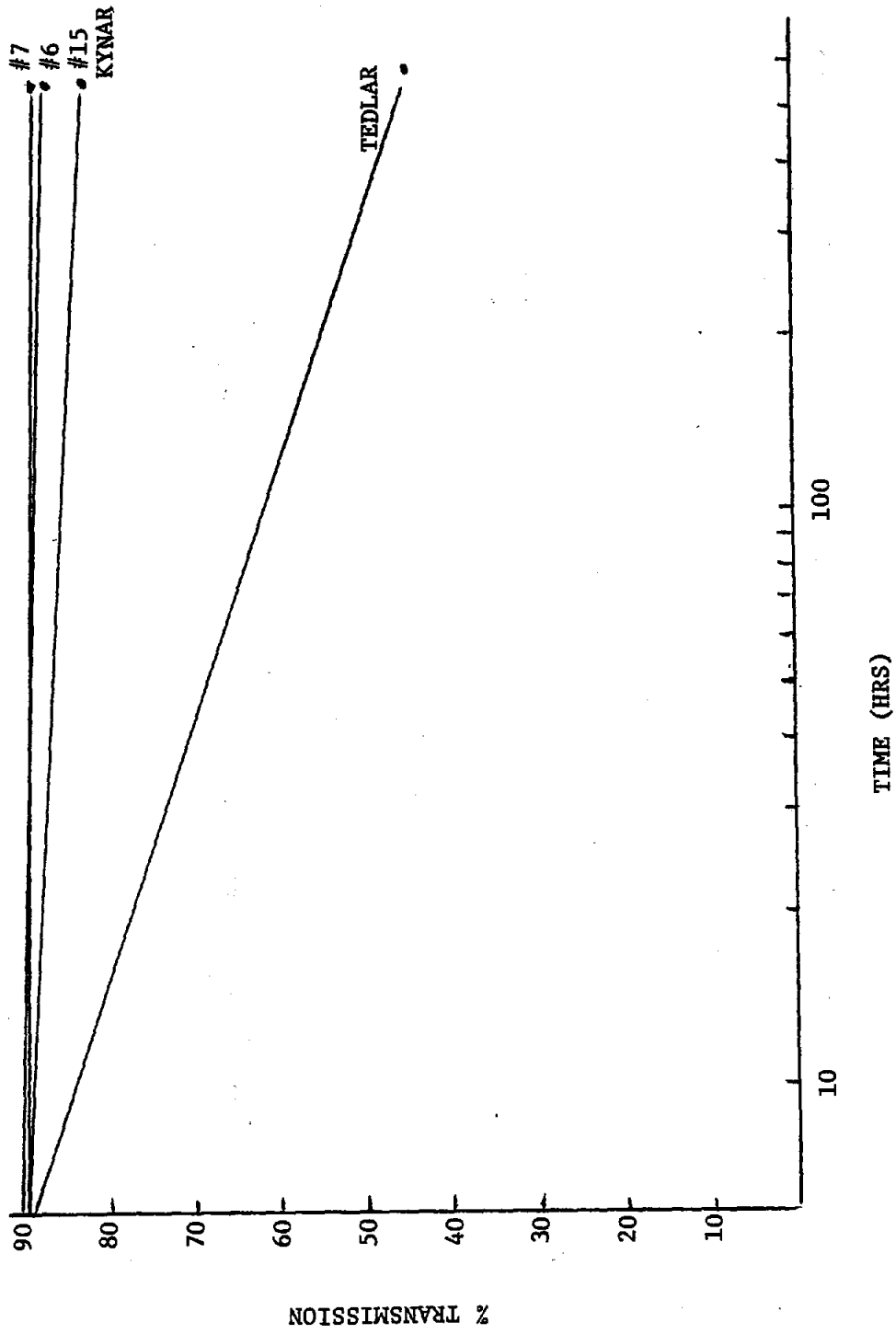


Figure 5.5-4. % Transmission vs. Hours in the Weatherometer

6.0 THERMOFORMING EXPERIMENTAL RESULTS

The formed domes were evaluated by measurement of transmittance, strength and geometry. Values were obtained for the different materials and for various forming conditions. For the environmental test domes the most promising forming conditions were used for each material.

6.1 POLYVINYLIDENE FLUORIDE (KYNAR)

Kynar was the primary material investigated in Phase B. Processing parameters were proven and test domes were fabricated in this Phase.

6.1.1 Kynar Process Experiments

The Phase B Kynar domes were formed using techniques developed in Phase A. Pre-heat times for 1.5 mm (60 mil) thick preforms were around 2.5 minutes. Domes were formed in around 15 to 20 seconds, with pressures up to 17.2 kPa (2.5 psi). The Kynar was found to be very temperature sensitive, i.e., there is only a 30°C (54°F) difference between the lowest forming temperature and T_m (melt temperature). Also, due to the high thermal expansion of the Kynar, wrinkles would form in the blank during preheating. This caused very unequal heating in the preform due to a combination of intermittent contact with the holder, which acted as a heat sink, and variations in the distance from heat source causing unequal heat input. These preforms could not be formed satisfactorily. A partial solution was to maintain tension on the preform during heating with a slight positive air pressure. This allowed the center section to bubble up and become warmer than the edges. Adequate domes were formed using this technique as shown in Figure 6.1.2-4, but they were limited in the maximum sizes obtainable.

Because of the sensitivity of Kynar to temperature, future studies should devote effort to assuring uniform temperature of the preform. Particular attention should be given to increasing temperature along the periphery of the preform where radiation heat sinks are visible to the Kynar. A more uniform preform temperature should allow greater expansion along the edges of the dome resulting in larger domes more spherical in shape.

6.1.2 Properties of Phase B Kynar Domes

Dome # 1/5/17 was selected to test for thickness variation, mechanical properties and transmittance because it exhibited a better shape than most. The thickness variation for the thermoformed dome is shown in Figure 6.1.2-1. A strip of material was cut from base to base through the polar cap and then a micrometer was used to determine thickness. Starting with a base thickness of 1.5 mm the dome remained quite thick for the first 10 cm and then thinned down from 1.2 mm to 0.35 mm within the next 5 cm. The material remained optically cloudy until it necked down to a thickness of 0.5 mm or less, which took place after the initial 12 to 13 cm. The top hemisphere was uniform in thickness, exhibiting a variation of ± 0.05 mm. It is expected that with more uniform heating of the preform, the Kynar near the base can be made thinner.

Specular transmittance of the Phase B Kynar dome was measured with a Beckman DK-2 spectrophotometer and a Gier Dunkle integrating sphere detector, using a scattering cone angle of 0.59° . Specular transmittance was calculated from spectral data using an air-mass-2 solar spectrum. Results are tabulated and shown in Figure 6.1.2-2. The top of the dome came close to meeting the requirement of 86% transmittance but the equator and the area near the base were measured at 75% and 62% transmittance, respectively. Upon investigating the reasons for low transmittance it was found that preform material had not been quenched following extrusion. Pennwalt determined in Phase A that for maximum transmittance, the material should be quenched in water immediately after extrusion.

Using the same Kynar dome (Dome # 1/5/17) the tensile yield, tensile ultimate, ultimate elongation, and yield strength* values were determined. Samples were cut from five positions; the polar cap, opposite sides on the equator, and opposite sides 15 cm up from the base. Each sample was divided into three vertical direction coupons and three horizontal direction coupons so that a total of 30 microtensile tests were performed.

* Yield strength is the load in kilonewtons per meter of film width at the 20% offset in the case of Kynar. In the case of all other films yield strength is the load at the proportional limit.

Actual profile of dome 1/5/17

Measurements taken every 15 cm along the circumference except at the base which are in 5.0 cm intervals

Thickness measurements are in millimeters

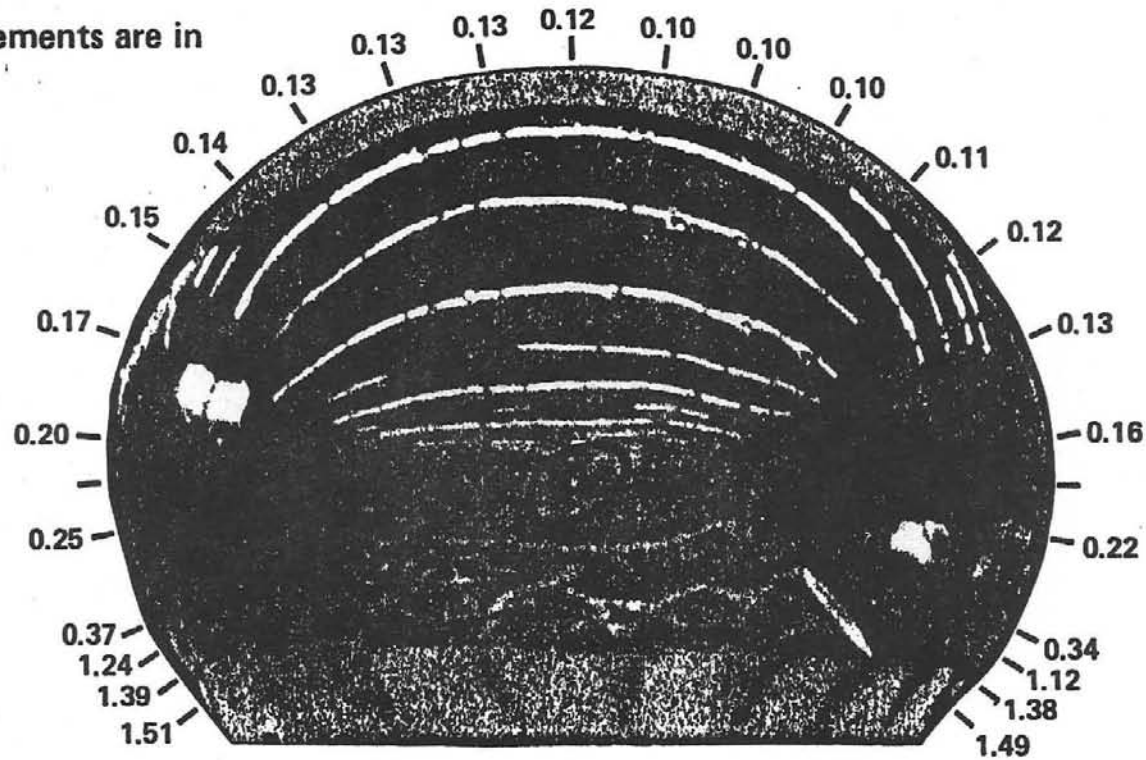
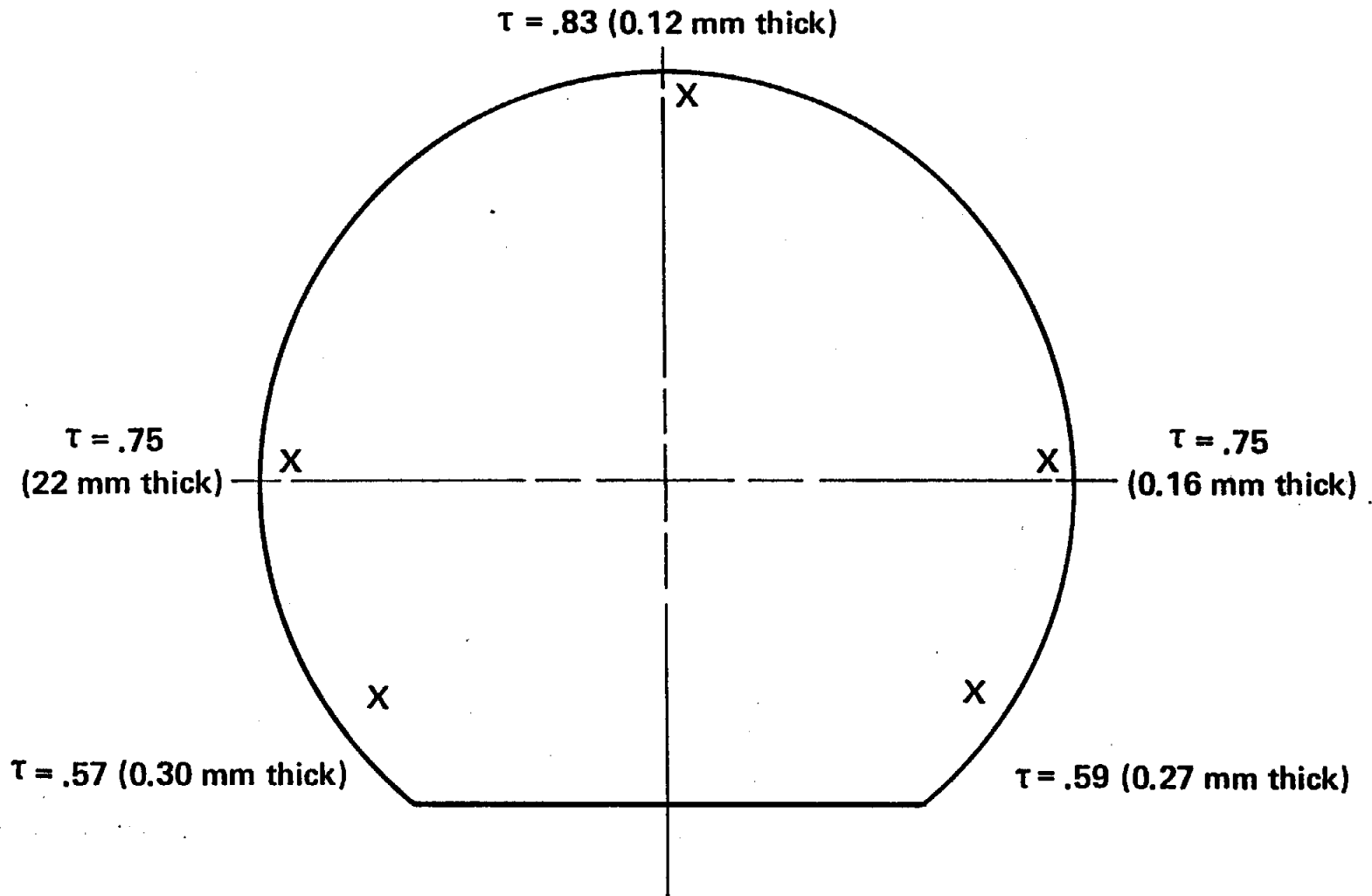


Figure 6.1.2-1. Thickness Versus Circumference of a Phase B Kynar Thermoformed Dome (No. 1/5/17)

0.59° cone angle integrated over solar spectrum (—air mass 2)



54

Figure 6.1.2-2. Specular Transmittance of Phase B Kynar Dome (No. 1/5/17) vs. Dome Position

The mean values were then computed for each direction and are shown in Table 6.1.2-1. The Kynar easily passed all strength requirements. The minimum yield strength was 10.5 kN/m which is 85% higher than the desired 5.7 kN/m. The minimum ultimate strength, which was 16.3 kN/m, is 72% higher than the desired 9.5 kN/m.

The shape of large domes formed in Phase B experiments was measured by optical comparison photography. Photographs were taken of Kynar Dome # 1/5/15 (which was one of the better shaped domes) with a grid backdrop. A best-fit circle was then concentrically traced over the picture. Figure 6.1.2-3 shows the profile of the Phase B Dome # 1/5/15 with a best-fit circle diameter of 1.27 m (50 inches). The difference between the radius of the best-fit circle and the actual radius was measured every 30°. The differences were converted to percentages of radius and then plotted. The dome was rotated in 45° increments to get an overall shape. The results of this test are shown in Figure 6.1.2-4 and show a maximum radius variation of +9.3% and -8.5%. Although slightly greater than the desired +5%, results were encouraging considering the early stages of process development.

6.2 POLYESTER (PETRA)

The majority of investigations on processing of polyester film were done in Phase A with Petra material. These included variations in heat flux, heating time, air pressure and air flow. In general these tests showed that: both shape and strength were improved by increasing the strain rate; preheating time and the resulting film temperature directly effect the blowing pressure and should be kept to a minimum for improved strength; and heating during forming affects the final shape of the dome. These are general results, and applied to all films tested. In Phase B these results were used to form a Petra dome approximately 1.8 m (6 ft) in diameter.

6.2.1 Polyester Process Experiments

To investigate the effect of strain rate on dome strength properties, domes were formed using various air flow rates. Domes formed at lower strain rates (forming time 120 seconds) had marginal properties. Domes formed in 35 seconds (strain rate = 276%/min), and 13 seconds (strain rate = 743%/min) all had appreciably better pro-

Position	Direction	Yield stress		Ultimate stress		Elongation %	Yield strength	
		MPa	kpsi	MPa	kpsi		KN/m	lbs/in
Polar cap	Vertical	90.3	13.1	138.6	20.1	77	12.9	74.6
	Horizontal	80.6	11.7	125.5	18.2	56	10.5	60.8
Equator	Vertical	115.1	16.7	160.6	23.3	99	18.2	105.2
	Horizontal	74.4	10.8	108.2	15.7	126	13.2	76.0
Equator	Vertical	110.3	16.0	157.2	22.8	101	20.6	118.9
	Horizontal	88.2	12.8	135.8	19.7	163	15.0	86.6
15 cm above base	Vertical	106.8	15.5	146.8	21.3	106	32.1	185.5
	Horizontal	47.6	6.9	73.8	10.7	288	17.4	100.3
15 cm above base	Vertical	108.2	15.7	154.4	22.4	110	32.9	190.0
	Horizontal	51.0	7.4	84.8	12.3	278	17.8	102.6
Base material (1.5 mm thick)	Vertical	48.9	7.1	52.4	7.6	344	78.7	454.4
	Horizontal	38.6	5.6	46.2	6.7	237	61.6	355.4

Table 6.1.2-3. Mechanical Properties of Phase B Kynar Dome (No. 1/5/17)

Profile of Kynar dome at 0°

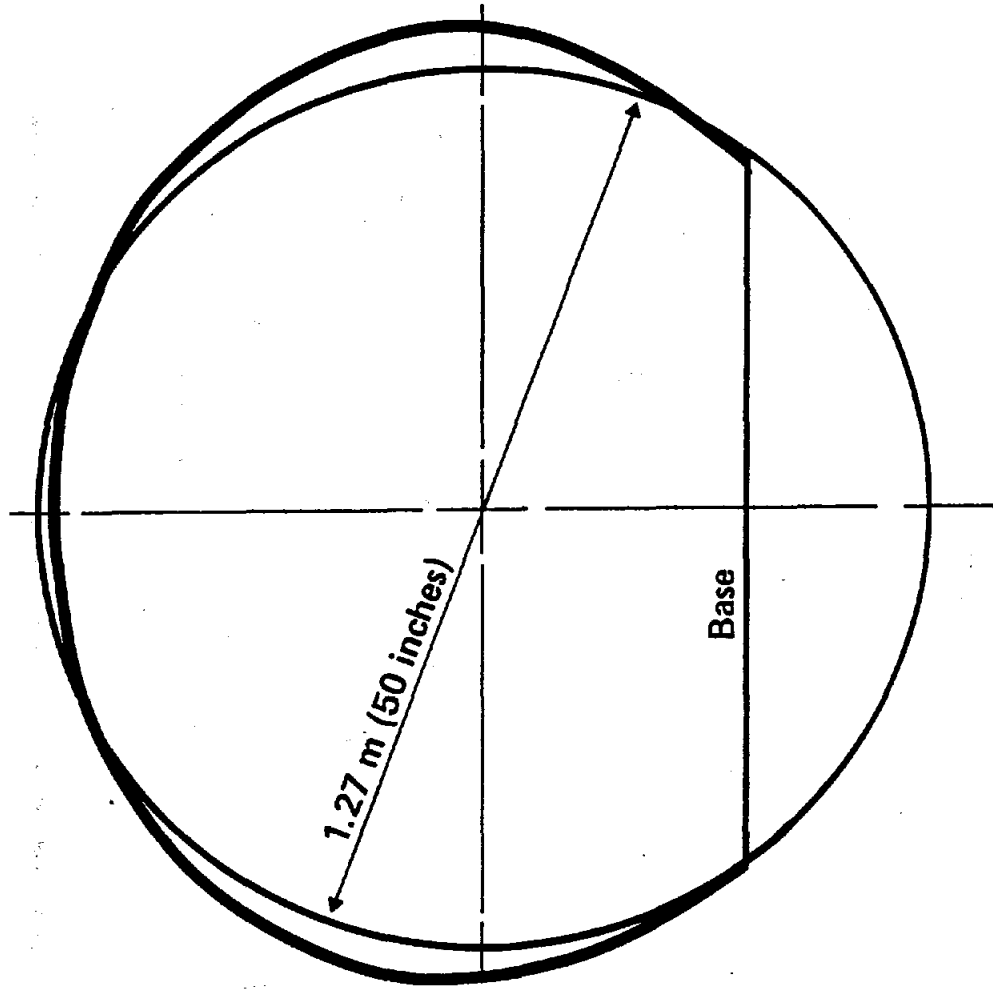


Figure 6.1.2-3. Best Fit Circle Concentrically Traced Over a Profile of a Phase B Kynar Dome

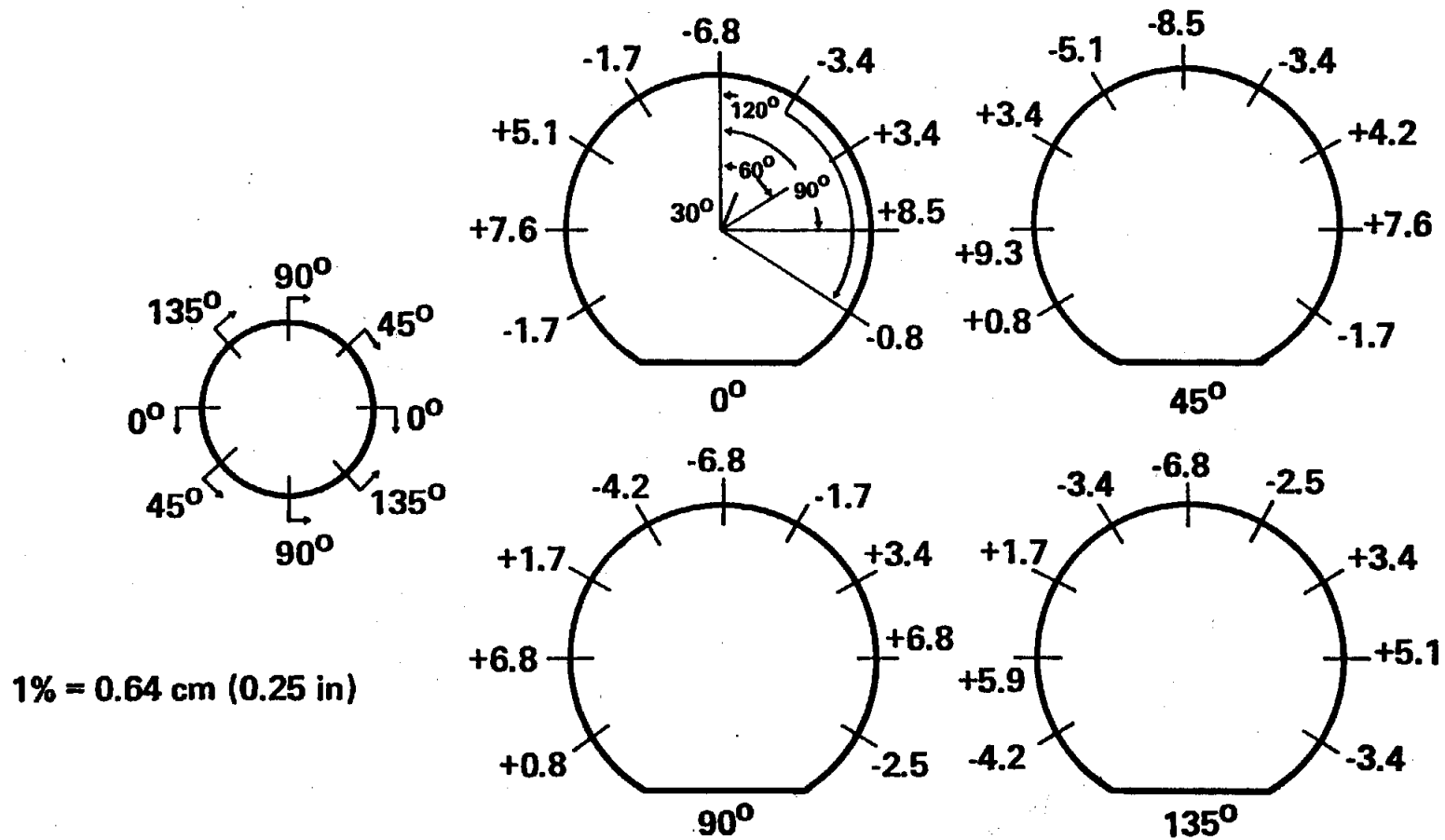


Figure 6.1.2-4. Deviation of Phase B Kynar Dome From a True Sphere Measured in %

perties. These results are compared in Table 6.2.1-1. The values were obtained from specimens taken from the top of the domes. Other values obtained at different dome heights and in both the vertical and horizontal directions all showed a similar relationship with strain rate.

The overall strain rate was calculated by first determining the area expansion ratio by dividing the final area of the formed dome by the initial area of the flat blank. For a theoretical dome with a base angle of 45° *, the area expansion ratio is equal to 6.83. By taking the square root of this area expansion ratio, an indication of the average linear strain can be obtained as follows, using a gauge length of one:

$$\text{Area Expansion Ratio} = \frac{\text{Final area}}{\text{Initial area}} = 6.83$$

$$\text{Linear Expansion Ratio} = \frac{\text{Final length}}{\text{Initial length}} = (6.83)^{1/2} = 2.61$$

$$\text{Linear Strain} = \frac{\text{Increase in gauge length}}{\text{Gauge length}} = 100 (2.61-1)/1 = 161\%$$

The film thickness does not remain constant over the entire surface of the dome during the forming operation. To obtain a better understanding of the local expansion ratios and film thicknesses in a formed dome, an analysis was made assuming the longitudinal stretch ratios were uniform. This assumption was based on a marked test dome in which equally spaced concentric circles marked on the preform ended up roughly as equally spaced latitude lines on the formed dome. The longitudinal stretch ratio was found to be 3.3. That is 1 unit stretched to 3.3 units. The linear strain or elongation would be equal to 2.3 or 230%. The latitudinal stretch ratios were calculated by dividing the radii of the expanded concentric circles by their initial radii. The results varied from a latitudinal stretch ratio of 3.2 near the top to 1.7 near the bottom of the dome. This is equivalent to 220% and 70% linear elongation, respectively.

If the longitudinal and latitudinal stretch ratios are multiplied together to obtain an equivalent area expansion ratio, which is then divided into the original film

* Base angle is defined as the angle between a vertical line passing through the geometric center of the dome, and the point of intersection between the dome and base plane.

Table 6.2.1-1. Effect of Strain Rate on Tensile Properties of Polyester Domes

Dome	Base Diameter (cm)	Forming Time (sec)	Ave. Strain Rate (%/min)	Tensile Properties—At Top Horizontal						
				Yield Stress		Ultimate Stress		Elongation %	Yield Strength	
				MPa	kpsi	MPa	kpsi		kW/m	lbs/in
10-19-6	25	120	80	69.6	10.1	101.4	14.7	169	3.0	17.2
10-31-16	25	35	276	91.7	13.3	167.5	24.3	90	4.2	23.9
10-31-15	25	13	743	98.6	14.3	174.4	25.3	62	4.5	25.7
3-5-21	107	12	805	73.8	10.7	133.8	19.4	115	4.8	278 27.8

thickness, an indication of the final thickness can be obtained. For a 0.5 mm (20 mil) initial film thickness, final thickness varies from 0.05 mm (1.9 mil) near the top to 0.09 mm (3.6 mil) near the bottom. These values agreed fairly well with actual measurements as shown in Figure 6.2.1-1. This figure shows the calculated distribution of stretch ratios and thickness variations, as well as the actual measurements made on a small dome formed in Phase A. The larger Phase B domes were also thin at the top and increased in thickness towards the base, but the change was more gradual through the middle of the dome. This can be seen in Figure 6.2.2-1.

The shape of the Petra domes were improved considerably by forming at a high strain rate. The domes formed at strain rates below 100%/min tended to be bulgy and squat. Dome # 10-19-6, formed in 120 seconds, had a radius 17% greater than a theoretical sphere of the same height. This is compared to a 7% variation in radius for Dome # 10-31-16, formed in 35 seconds. This also held true for the larger Phase B domes where Dome # 1-5-22, formed in 12 seconds, had a radius only about 1.5% greater than theoretical.

6.2.2 Properties of Phase B Petra Domes

The same tests that were performed on the Kynar thermoformed domes were repeated on large Petra domes using the same procedures. Dome # 3-5-21 was selected for evaluation of its mechanical and optical properties because it exhibited one of the better shapes. The thickness variation vs. circumference of the Phase B Petra AXB dome is shown in Figure 6.2.2-1. The dome exhibited very uniform thickness (± 0.015 mm) once the initial necking down near the base plane had taken place.

Mechanical properties were determined from samples cut at the polar cap, opposite sides at the equator, and 15 cm up from the base. The results of the microtensile tests, shown in Table 6.2.2-1, indicate that the Petra dome did not achieve the desired yield strength of 5.7 kN/m and ultimate strength of 9.5 kN/m. Increased strength can be achieved in future work by increasing preform thickness from 0.5 mm (20 mil) to 0.75 mm (30 mil) or thicker.

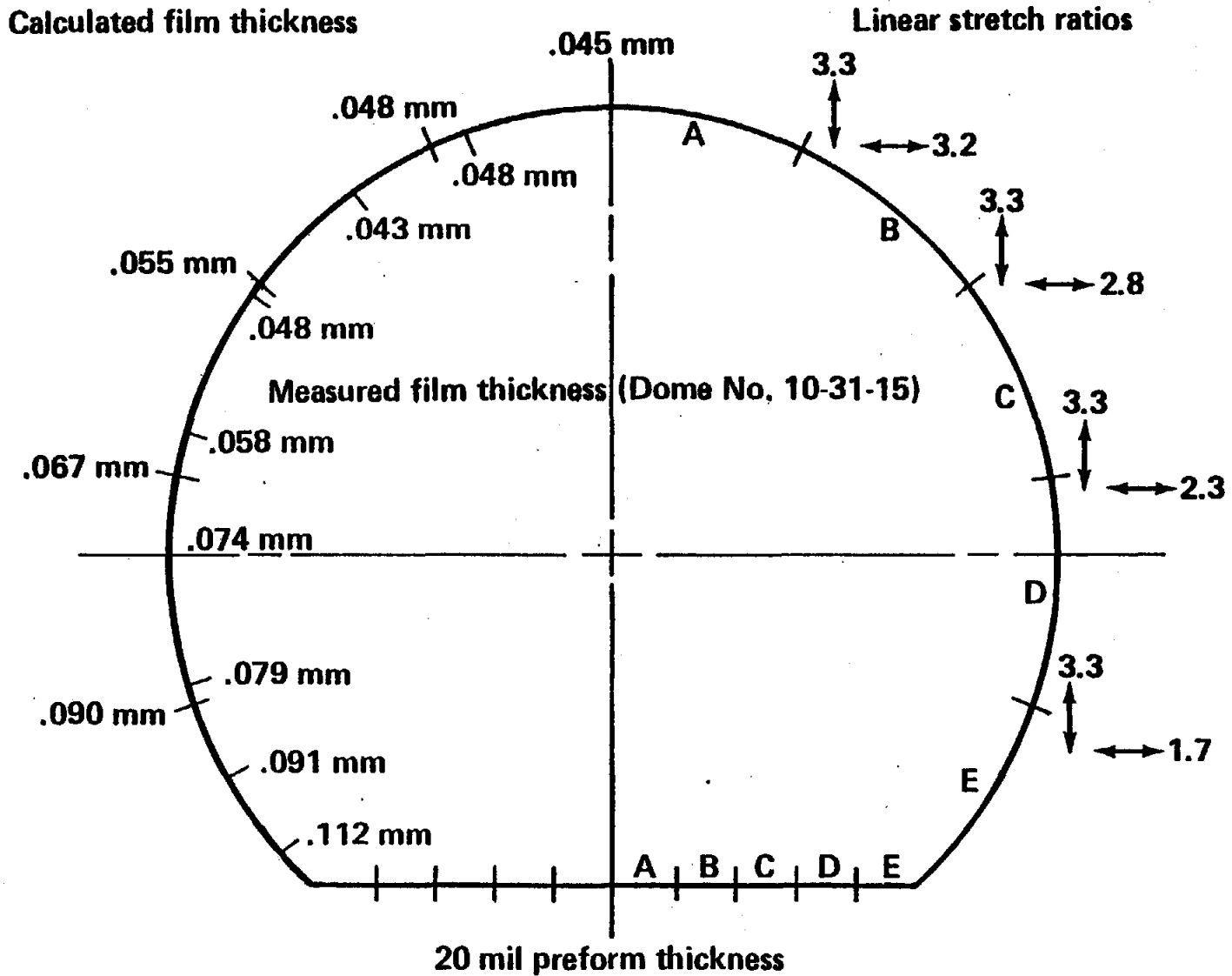


Figure 6.2.1-1. Calculated and Measured Stretch Ratios and Film Thickness Distribution for Polyester Dome Formed in Phase A

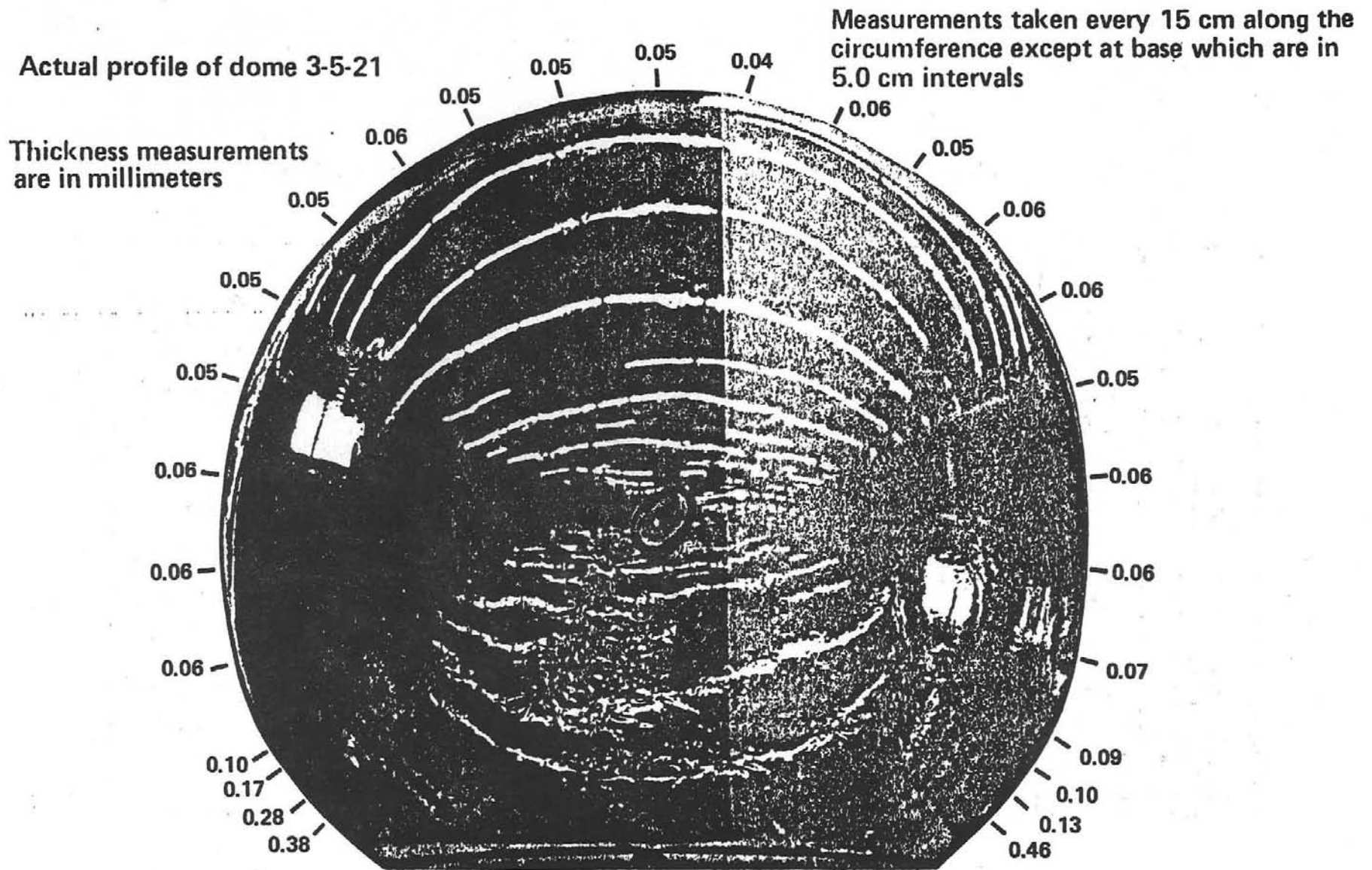


Figure 6.2.2-1. Thickness Distribution of a Phase B Petra AXB Thermoformed Dome (No. 3/5/21)

Position	Direction	Yield stress		Ultimate stress		Elongation %	Yield strength	
		MPa	kpsi	MPa	kpsi		kN/m	lbs/in
Polar cap	Vertical	65.5	9.5	100.0	14.5	171	3.8	21.9
	Horizontal	73.8	10.7	133.8	19.4	115	4.8	27.8
Equator	Vertical	84.8	12.3	143.4	20.8	85	4.7	27.0
	Horizontal	64.1	9.3	93.1	13.5	172	3.9	22.3
Equator	Vertical	91.0	13.2	138.6	20.1	72	6.2	35.6
	Horizontal	60.0	8.7	83.4	12.1	199	3.9	22.6
15 cm above base	Vertical	104.8	15.2	151.0	21.9	51	10.0	57.8
	Horizontal	51.0	7.4	97.9	14.2	269	3.8	22.2
15 cm above base	Vertical	133.1	19.3	177.2	25.7	42	12.7	73.3
	Horizontal	47.6	6.9	64.8	9.4	314	4.7	26.9

Table 6.2.2-1. Mechanical Properties of Phase B Petra AXB Dome (No. 3/5/21)

Transmittance values measured on large Petra domes near the base, equator, and polar cap are shown in Figure 6.2.2-2. Respective values at the base and equator exceeded the desired transmittance of 86% at 0.14° scattering cone angle (633 nanometer wavelength). Transmittance at the pole was 3% lower than the goal. Lower transmittance at the polar cap was believed to be caused by localized overheating of the preform which led to crystal growth in the material. It is believed this problem can be eliminated by creating a uniform thermal environment during heating.

The shape of a Phase B Petra dome was measured similarly to the large Kynar dome. Petra Dome # 1-5-22 was chosen to evaluate because it was the largest one blown. A best-fit circle of 1.73 cm (68 in) was then concentrically traced over the picture as shown in Figure 6.2.2-3. The differences between the actual radius and the best-fit radius are shown in Figure 6.2.2-4. The geometry of the dome fell within the desired $\pm 5\%$ radius variation.

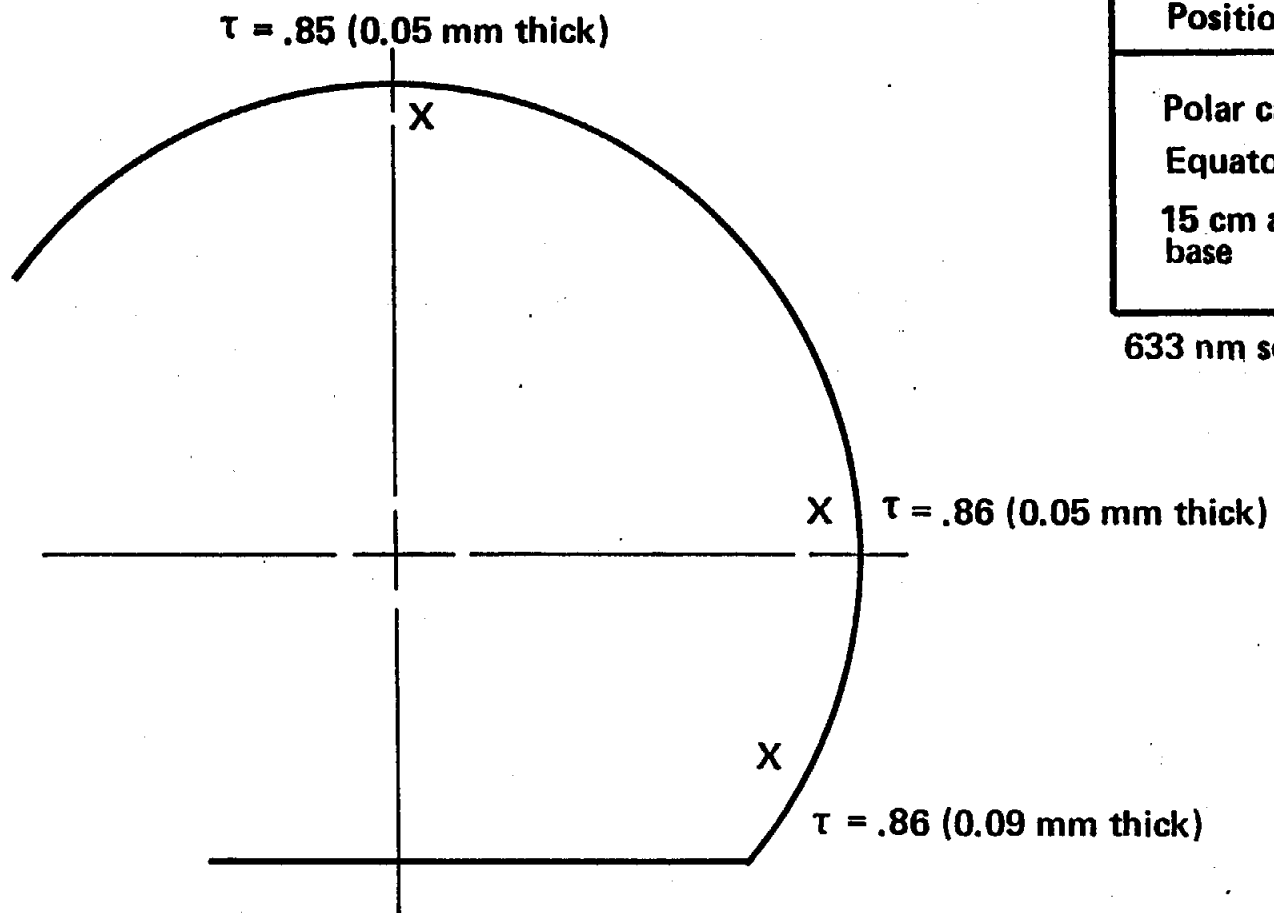
6.3 OTHER MATERIALS

In phase A several other film materials were investigated as potential one piece domes. These included other polyesters, cellulose acetate butyrate, polyvinyl fluoride, and ethylene-chlorotrifluoroethylene.

6.3.1 Polyester (Meliform and Melinex-0)

Meliform was used to prepare one-piece test domes and domes with heat sealed joints. The Melinex-0 was used to form laminated domes and domes with high area expansion ratios. The mechanical properties of the Meliform dome are given in Table 7.2-4. The high expansion dome tested was formed at an average strain rate of 500% per minute. It was formed from a blank 1.27 mm (50 mils) thick. The expansion ratio was approximately 27, with the dome height of 63.5 cm (25 in) and a diameter of 68.6 cm (27 in).

All of the Meliform domes had a slight cloudiness after forming. An unsuccessful attempt was made to eliminate cloudiness by trying various preheat cycles and forming times. These experiments resulted in a loss in transmission as can be seen in Table 7.2-6. The Melinex-0 preform material had a yellow appearance which tended to disappear during forming (probably by thinning).



**0.59° cone angle integrated
solar spectrum**

Position	Cone Angle			
	.08	.14	.28	.59
Polar cap	.80	.83	.84	.85
Equator	.86	.87	.87	.87
15 cm above base	.87	.87	.88	.88

633 nm source with various cone angles

Figure 6.2.2-2. Transmittance of Phase B Petra AXB Dome (No. 3/5/21)

Profile of Petra AXB dome at 0°

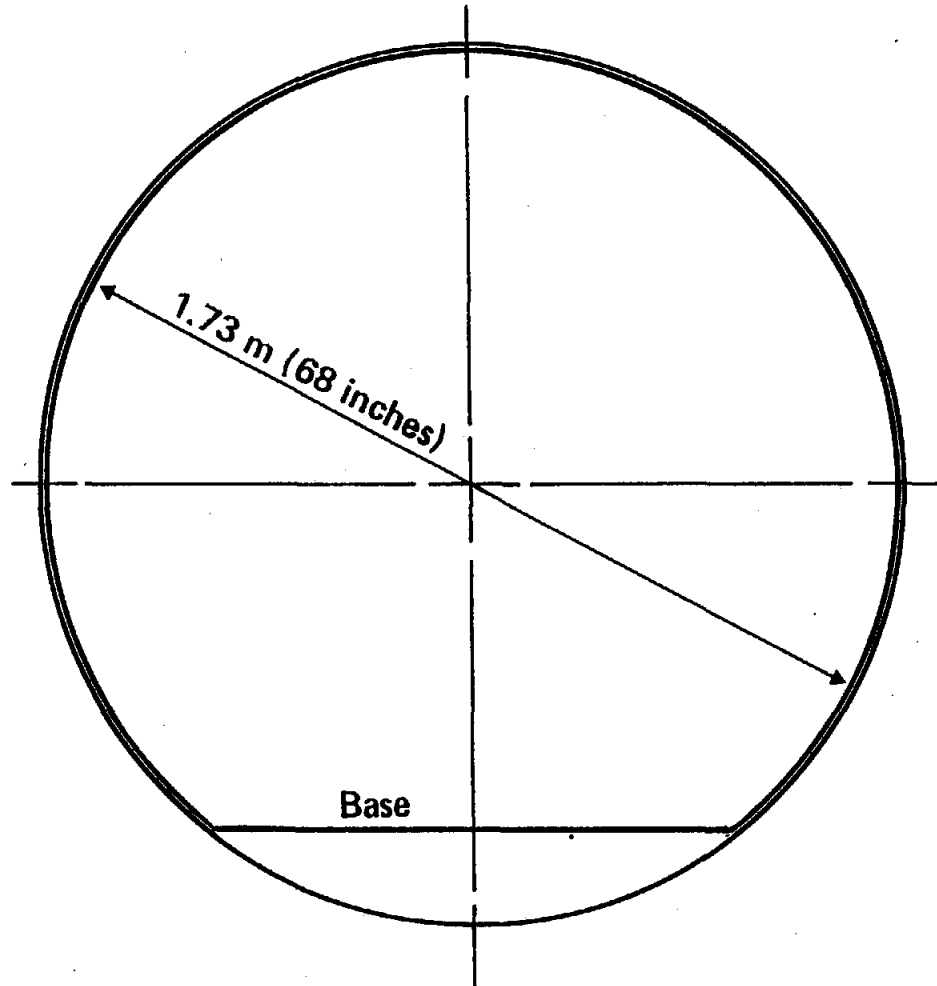


Figure 6.2.2-3 Best Fit Circle Concentrically Traced Over a Profile of a Phase B Petra AXB Dome From a True Sphere Measured in % (No. 1/5/22)

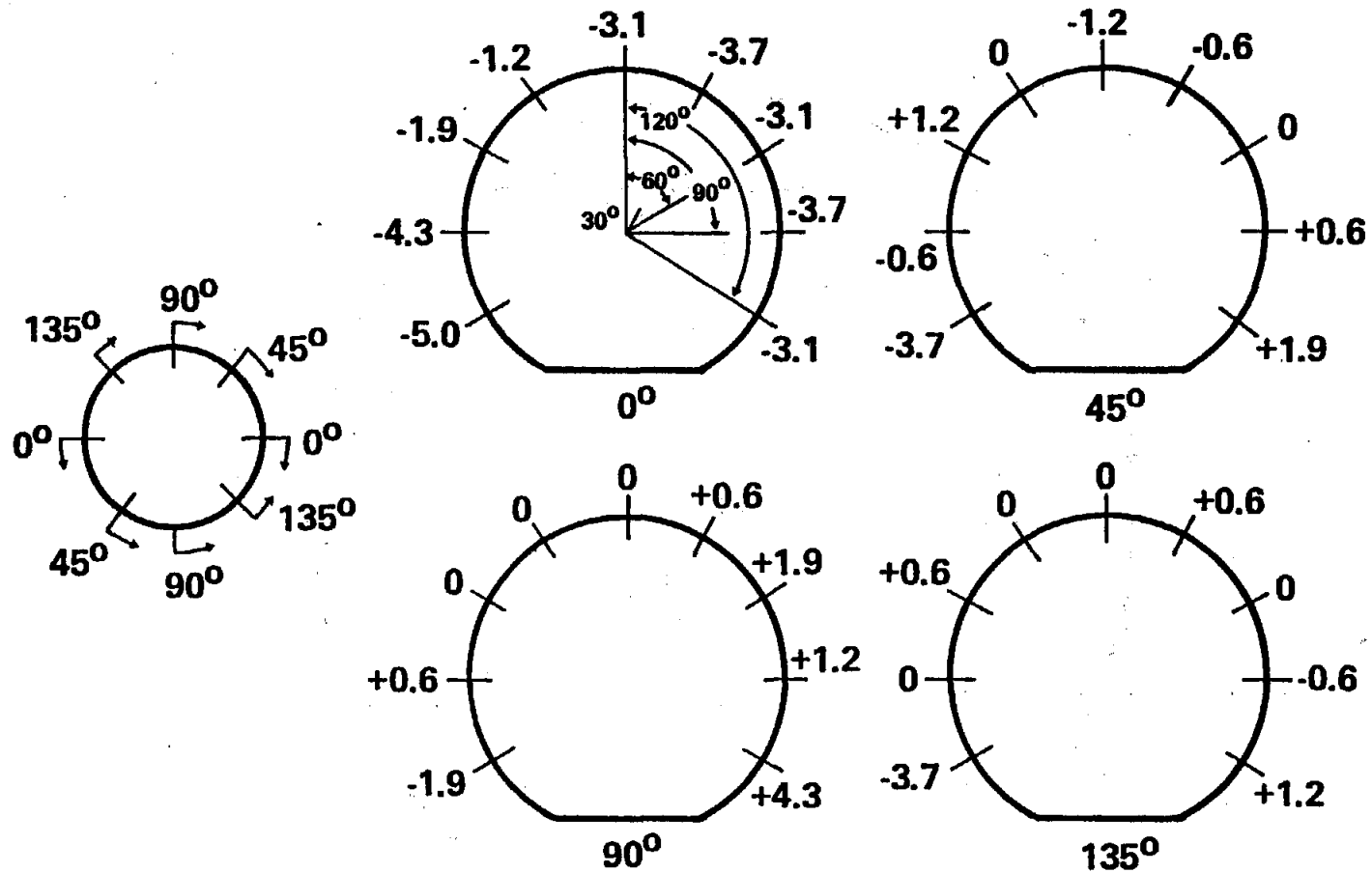


Figure 6.2.2-4. Deviation of Phase B Petra AXB Dome From a True Sphere Measured in % (No. 1/5/22)

6.3.2 Polyester (PETG-7821)

One piece test domes and domes with heat-sealed joints were formed from PETG-7821. All of these were formed at high strain rates. The mechanical values are given in Table 7.2-3. Transmittance values are given in Table 7.2-6. This material formed very similar to Petra.

6.3.3 Cellulose Acetate Butyrate (UVEX)

The cellulose acetate butyrate material used was thicker than desired for thermoforming domes. Because of this and the limited number of samples available, no satisfactory thermoforming process was developed. The maximum size obtained was slightly larger than a hemisphere. Those that were blown with increased temperature or pressure developed thin spots with resulting uneven shape. Some surface deterioration was also noted on blanks with long preheat cycles. The samples with shorter preheat cycles showed good clarity, and fairly uniform thicknesses were obtained for the hemisphere shape.

6.3.4 Polyvinyl Fluoride (Tedlar)

The Tedlar tested was a special formable grade having minimum orientation. It was, however, very thin (0.04 mm) for dome thermoforming preforms. A hemisphere was the largest shape successfully formed. One dome reached approximately 22 cm (9 in) in height before failure. This was equivalent to an area expansion ratio of 4. The theoretical area expansion ratio for a hemisphere is 2, and for a 45° base angle dome is 6.8. The domes had good clarity, but a sharp transition could be seen between stretched and partially stretched material. No tests were made on material as no satisfactory domes were formed.

6.3.5 Ethylene-Chlorotrifluoroethylene (Halar)

The Halar films used were relatively thin (0.25 mm) for thermoforming and appeared to have a residual orientation that prevented the forming of a uniform dome. Any domes that were formed past a hemisphere had definite bulges and thin spots that generally resulted in failure. Even the hemisphere size domes had irregular thin areas. These areas, however, were very clear compared to the thicker areas. There was no indication of crystallinity, even with the preforms exposed to a long preheat step. Unoriented thicker material for preforms would be necessary if satisfactory domes are to be formed from this material.

6.4 PREFORM PREPARATION

With domes larger than approximately 1.85 m (6 ft) in diameter the size of the preforms required exceed the width of presently available film materials. For example, a 9.69 m (31.8 ft) diameter dome with a 45° base angle would require a preform diameter of 7.3 m (24 ft). Accordingly, an investigation was conducted to select and evaluate preferred processes for preparation of large preforms.

In Phase A, two approaches to fabricating multi-piece thermoforming blanks were evaluated. In one, a simple overlapping heat-seal was used. In the other, a laminate was made by fusing plies of film together with butt joints on the inner plies. Polyester films were used to evaluate these techniques. The preforms fabricated in Phase A were approximately 0.3 m (1 ft) in diameter.

In Phase B, where preforms 1.2 m (4 ft) in diameter were used, two types of joints and two ways of laminating were investigated. The joints consisted of an overlap joint made in a press, and a fused butt weld which was pressed flat. The laminating techniques were press-laminated, and roll lamination. In the latter the samples were preheated prior to lamination. All of the Phase B investigations utilized Kynar film. Results of these studies, discussed below, showed that it is considered very feasible to fabricate large preforms by either press laminating or heat sealed joints. The latter can be accomplished by either overlapping or butt welding.

It is not possible to extrude full-scale one-piece preforms at the present time due to size limitations of existing extrusion equipment.

6.4.1 Heat Sealing Experiments

Overlapping heat sealed joints with the 0.51 mm (20 mil) polyester materials were made in Phase A using an impulse sealer heating on the top only. With thick materials this increased sealing time to the point where some materials became opaque due to crystal growth in the seal area. The strength across joints in formed domes was generally within 10% of the comparable base material. The shape of domes was comparable to domes without seams, except for a small area adjacent to the seam.

In Phase B, 1.52 mm (60 mil) thick Kynar film was joined with an overlapping heat seal using a press to provide the heat and pressure. A very good fused joint was obtained but the remaining sheet material became wavy due to not being held flat in the press. In trying to thermoform these wavy preforms, thin areas were overheated and failed when pressure was applied. No domes could be formed with these preforms.

Despite the above problem, heat sealing an overlapping joint is still considered a feasible way to fabricate full scale blanks. The equivalent of a long narrow press could be used at each joint area to fuse only the overlapping portion of the film. This approach would be very adequate for Kynar film. For polyester film the added thermal cycle could cause local crystal growth. A press or heat sealer 7.3 m (24 ft) long and approximately 0.15 m (0.5 ft) wide is very feasible.

6.4.2 Lamination Experiments

Laminated preforms were made using both polyester and Kynar films. The polyester laminates were 4 ply and the Kynar, 6 ply. Both had butt joints on the inner plies. The polyester laminates used 0.127 mm (5 mil) films. In Phase A these were laminated and fused by vacuum bagging and using the infrared oven for the fusion heat source. By this technique, adequate fusion was obtained to allow the forming of a dome with butt joints on the inner ply. These joints did not separate or delaminate during forming. However, with the hand lay-up techniques used, it was not possible to remove all of the air between laminations.

In Phase B, Kynar was successfully laminated using a press. Six 0.25 mm (10 mil) plies were assembled using butt joints on the 4 inner plies. The resulting laminates were free of any air pockets or voids. Domes with diameters of around 1.2 m (4 ft) were formed with those laminates. Only a slight trace of any of the butt joints could be found in the formed dome.

An attempt was also made to laminate Kynar using a safety glass laminating line at Binswanger Mirror Company in Tempe, Arizona. The Kynar plies were placed between two pieces of glass and then passed sequentially through an oven, a roll, a second oven, and finally through a final roll. It was possible to heat the Kynar film to fusion temperature but it was not possible to remove all of the air. An autoclave cycle was tried on some of the samples without success.

A press appears to be the best way for laminating the film preforms. Westlake Plastics Company, who laminated the Kynar for this program, considers press laminating the most promising way of obtaining large preforms. The largest existing press capability is a "4000 ton" press with a custom design bed size of 6.1 m x 6.1 m (20 ft. x 20 ft.). This press will produce sufficient pressure to laminate the Kynar. With a 7.3 m (24 ft) diameter bed it will have 827 kN/m^2 (120 psi) pressure. The Kynar was laminated using 69 kN/m^2 (10 psi).

6.4.3 Butt Welding Experiments

Kynar samples, 1.52 mm (60 mil) thick, were butt welded, trimmed, and formed in Phase B. The joining process consisted of heating the edges of the film, joining, and then locally pressing. The resulting joint was void free and formed adequately. This process is one of the more promising for making full scale blanks.

6.4.4 Wide Extrusions

The present capability for extruding Kynar and unoriented polyester is 1.27 m (50 in). The maximum known width of a sheet extrusion plant is 3.4 m (11.1 ft). The extrusion width required for a full scale dome formed with a 45° base angle is 7.3 m (24 ft). Discussions with manufacturers indicated that equipment to handle extrusions of this width is possible, but not practical for small production rates. The width of the extrusion die and the diameter of the extruder would both have to be considerably larger than any presently available. The take-off and cooling rolls could utilize paper machine rolls which are up to 9.6 m (30 feet) wide.

An alternative approach to full-scale preforms is to expand domes to a higher ratio (smaller base angle) and use smaller preform. The smaller preform would, however, have to be thicker to obtain the same final dome thickness. For a preform 3.0 m (10 ft) in diameter the thickness would have to be increased 500%, and the dome expanded to a ratio of about 40 to 1, with an 18° base angle. This might be possible with polyester materials which have been formed to an area expansion ratio of 27. Kynar would require additional process work since it has been limited to expansion ratios of about 7.

7.0 DESERT EXPOSURE TESTS

In Phase A, desert exposure testing was initiated on domes of the most promising materials, joining techniques and lamination approaches. The purpose of this testing was to verify the weatherability of the various materials and processes. Table 7.0-1 provides a list of the five materials selected. Also included are the supplier names, number of domes installed, and types of joining and lamination processes being tested.

7.1 APPARATUS

A total of 26 sample domes of nominal 35.5 cm (14 in) diameter, except for the 61 cm (24 in) Kynar domes were prepared and installed at the Desert Sunshine Exposure Test Facility (D.S.E.T.) near Phoenix, Arizona. Twenty-five domes were mounted on a steel rack 1.22 m (4 ft) above ground level. An additional dome (PETG 7821 one piece) was mounted 3.7 m (12 ft) above ground for purposes of determining any differences in effects of particular abrasion and deposition. Figure 7.1-1 depicts the domes and test apparatus. Figure 7.1-2 is a photograph of the overall set-up and Figure 7.1-3 is a close-up photograph showing two domes, the gas supply bottle, regulators, and delivery lines.

Domes were clamped to base plates on the rack utilizing the preform flange at the bottom of the dome, a tie-down ring-flange and gaskets. The domes are inflated with air which is delivered by lines running from a compressed air bottle to fittings penetrating the base plates. Each dome is provided with a small hand valve that allows individual on-off control as well as acting as a low-flow restriction in the event one or more domes are damaged. A water manometer is provided to monitor supply line pressure. A pressure of 6.9 kPa (1 psi) was maintained in the domes. This provided a film stress approximately equal to that of a full scale dome.

7.2 RESULTS OF DESERT EXPOSURE

After 5 months of exposure, 5 domes were removed for evaluation of optical and mechanical properties. During these 5 months, the domes were exposed to 53,600 Langleys (1 Langley = 1 cal/cm²), hail, dust storms, freezing weather, and winds in excess of 13.4 m/s (30 mph).

Table 7.0-1. Environmental Exposure Test Materials

Material	Supplier	Number of domes installed	Process
Kynar 460 – Polyvinylidene Fluoride (Blown by Pennwalt)	Pennwalt	2	One piece
Petra AXB – U/V stabilized polyester	Allied Chem.	3 3 3	One piece Heat sealed joint 4 ply-butt joints
PETG 7821 – Unstabilized polyester	Eastman	3 3	One piece Heat sealed joints
Meliform – Unstabilized polyester	ICI Americas	3 3	One piece Heat sealed joints
Melinex-O – U/V stabilized polyester	ICI Americas	3	4 ply-butt joints

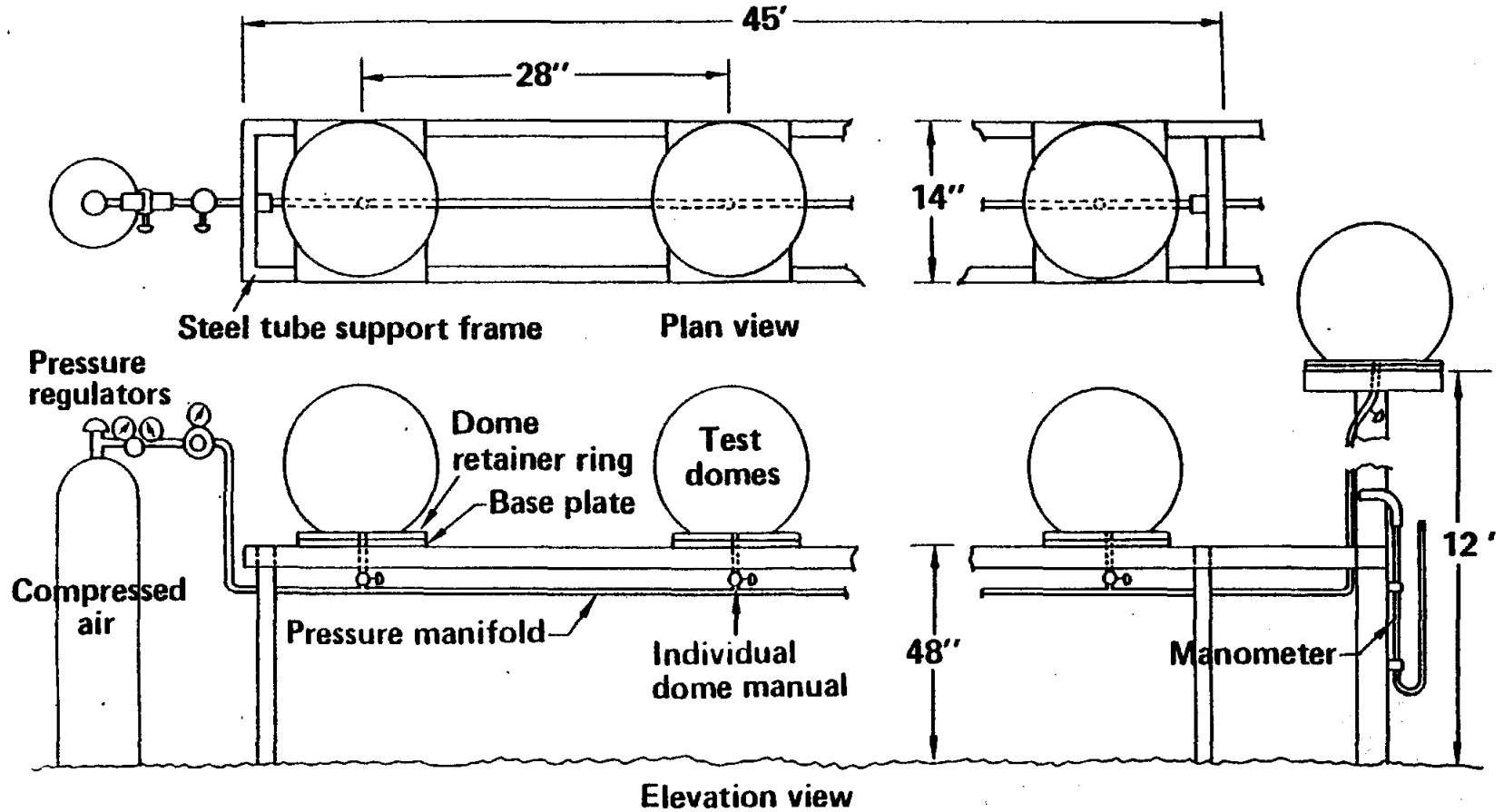


Figure 7.1-1. Enclosure and Support Stand



Figure 7.1-2. Photograph of Enclosures and Support Stand

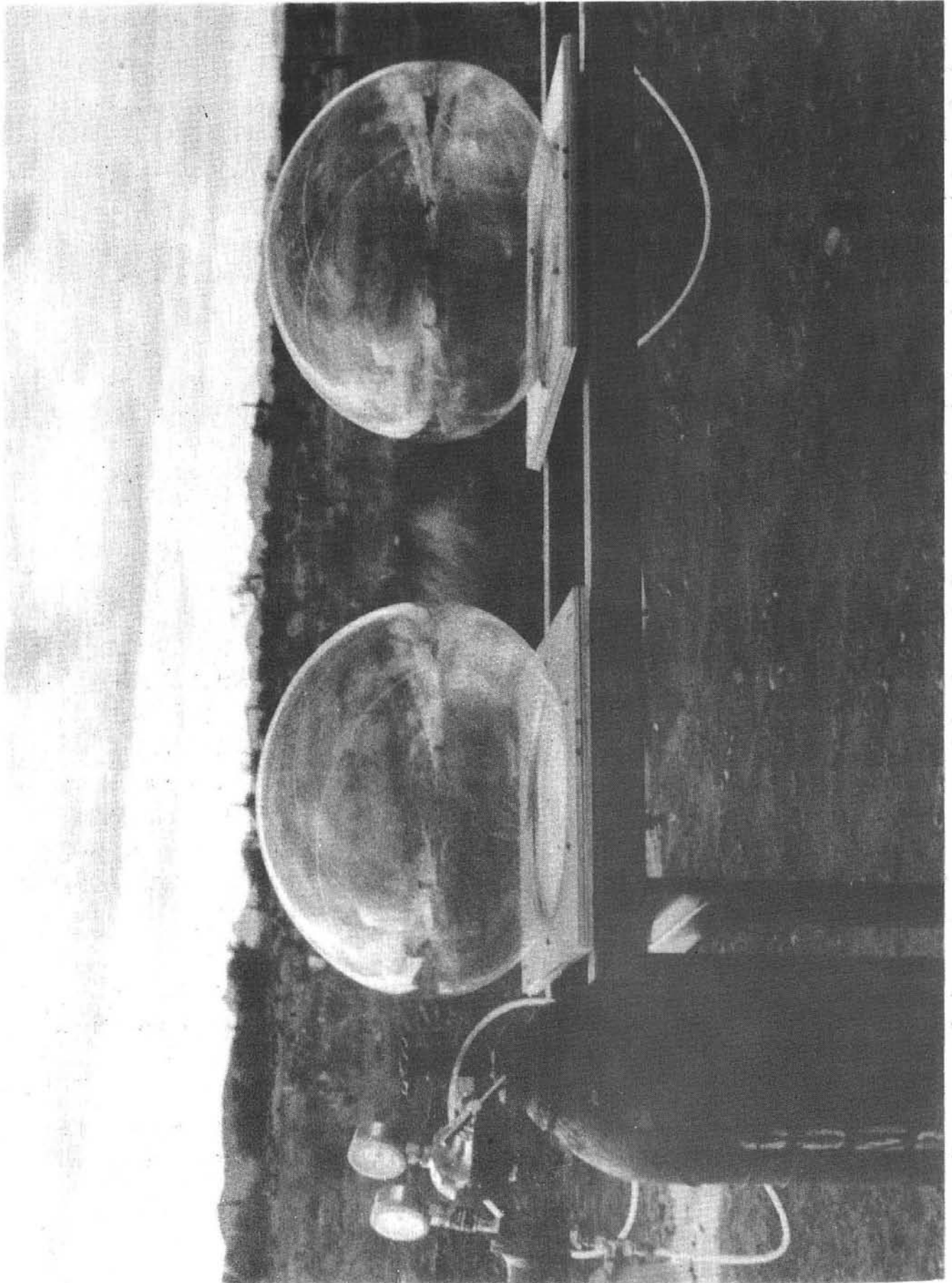


Figure 7.1-3. Photograph of Domes and Test Hardware

The following domes were removed for testing: Meliform, PETG 7821 with a heat sealed joint, Petra AXB, Petra AXB with a heat sealed joint, and a Petra AXB 4 ply laminated dome. During the first 5 months of exposure there were several dome failures which prevented testing of all the various domes. Some of the failures were caused by handling and installation. Two of the 3 Melinex domes failed in this manner and were damaged beyond repair. The third dome was left for further exposure. The other failures were environmental related. Every polyester dome whose failure was environmental related was either formed with a heat-sealed joint, or was made of unstabilized polyester.

The first PETG 7821 dome installed on the 3.7 m tower failed after 2 weeks. A second PETG 7821 dome (previously on the horizontal rack for 4 months) was installed on the tower and was torn beyond repair after one and a half months. These failures (cause unknown, but likely material becoming brittle) prevented study of differences in abrasion and deposition.

Kynar domes were left in the field for longer exposure because previous studies showed negligible loss of performance after 5 months.

The mechanical properties of Phase A thermoformed domes after 5 months exposure, are compared to their control values in Tables 7.2-1 through 7.2-5. The unstabilized polyesters (Meliform and PETG 7821) showed a substantial reduction in elongation values and a small increase in yield strengths. This is a normal trend for unstabilized polyesters. The Meliform dome showed an average elongation drop of almost 30%, and the PETG 7821 dome showed a drop of almost 50%. The elongation of the seam at the polar cap of the PETG dome decreased from 57% to only 3% during the 5 month outdoor exposure.

The Petra AXB domes (which are stabilized) showed little if any degradation in their mechanical properties. The only change of real significance was a decrease in elongation from 54% to 21% across a heat sealed joint at the pole.

Table 7.2-6 compares the optical properties of the domes before being sent to D.S.E.T., "as received" after 5 months exposure and after being cleaned. The

Exposure	Position	Direction	Yield Stress		Ultimate Stress		Elongation %	Yield Strength		
			MPa	kpsi	MPa	kpsi		kN/m	lbs/in	
Control	Polar cap	Vertical	95.1	13.8	160.6	23.3	66	4.3	24.8	
		Horizontal	93.1	13.5	133.8	19.4	69	4.4	25.0	
		Seam	64.8	9.4	83.4	12.1	54	3.8	21.8	
	Equator	Vertical	96.5	14.0	150.3	21.8	74	5.6	32.1	
		Horizontal	75.1	10.9	102.0	14.8	162	4.7	27.1	
	1 cm up from base	Vertical	116.5	16.9	156.5	22.7	67	10.7	60.9	
		Horizontal	51.7	7.5	62.7	9.1	357	6.0	34.1	
	5 months at D.S.E.T. (53,600 langley's)	Polar Cap	Vertical	102.7	14.9	160.6	23.3	79	3.9	22.4
			Horizontal	115.8	16.8	131.0	19.0	87	4.1	23.5
Seam			97.2	14.1	97.2	14.1	21	3.4	19.7	
Equator		Vertical	109.6	15.9	161.3	23.4	83	5.5	31.8	
		Horizontal	88.3	12.8	115.8	16.8	187	4.2	24.3	
1 cm up from base		Vertical	126.9	18.4	187.5	27.2	78	8.9	51.5	
		Horizontal	71.0	10.3	71.0	10.3	353	6.3	36.1	

Table 7.2-1. Mechanical Properties of a Phase A Petra AXB Dome With a Heat-Sealed Joint Before and After Desert Exposure

Exposure	Position	Direction	Yield Stress		Ultimate Stress		Elongation %	Yield Strength	
			MPa	kpsi	MPa	kpsi		kN/m	lbs/in
Control	Polar Cap	Vertical	75.1	10.9	105.5	15.3	95	4.3	24.8
		Horizontal	82.7	12.0	139.3	20.2	72	4.1	23.6
	Equator	Vertical	89.6	13.0	125.5	18.2	89	5.5	31.3
		Horizontal	64.8	9.4	114.4	16.6	99	4.2	23.8
	1 cm up from base	Vertical	120.7	17.5	154.4	22.4	56	13.1	74.7
		Horizontal	46.9	6.8	59.3	8.6	324	6.7	38.3
5 months at D.S.E.T. (53,600 langleys)	Polar cap	Vertical	96.5	14.0	142.7	20.7	68	3.9	22.4
		Horizontal	104.1	15.1	151.7	22.0	57	4.2	24.2
	Equator	Vertical	108.2	15.7	180.0	26.1	71	6.0	34.5
		Horizontal	84.1	12.2	122.0	17.7	126	4.9	28.1
	1 cm up from base	Vertical	140.7	20.4	220.6	32.0	64	9.6	55.1
		Horizontal	53.1	7.7	66.2	9.6	318	6.0	34.7

Table 7.2-2. Mechanical Properties of a Phase A Petra AXB Dome Before and After Desert Exposure

Exposure	Position	Direction	Yield Stress		Ultimate Stress		Elongation %	Yield Strength		
			MPa	kpsi	MPa	kpsi		kN/m	lbs/in	
Control	Polar cap	Vertical	127.6	18.5	198.6	28.8	61	3.7	21.4	
		Horizontal	62.1	9.0	97.9	14.2	67	2.9	16.8	
		Seam	46.2	6.7	46.2	6.7	57	3.4	19.3	
	Equator	Vertical	58.6	8.5	86.9	12.6	88	3.9	22.5	
		Horizontal	44.1	6.4	49.6	7.2	220	4.6	26.2	
	1 cm up from base	Vertical	88.9	12.9	133.1	19.3	80	14.3	81.5	
		Horizontal	51.7	7.5	68.9	10.0	160	3.1	17.9	
	5 months at D.S.E.T. (53,600 langleys)	Polar cap	Vertical	99.3	14.4	105.5	15.3	47	3.2	18.7
			Horizontal	97.9	14.2	109.6	15.9	42	3.7	21.3
Seam			102.0	14.8	102.0	14.8	3	3.1	17.8	
Equator		Vertical	108.9	15.8	137.2	19.9	39	6.0	34.8	
		Horizontal	71.0	10.3	76.5	11.1	74	3.6	20.6	
1 cm up from base		Vertical	123.4	17.9	168.9	24.5	35	11.5	66.2	
		Horizontal	49.6	7.2	53.1	7.7	149	4.4	25.2	

Table 7.2-3. Mechanical Properties of a Phase A PETG 7821 Dome Before and After Desert Exposure

Exposure	Position	Direction	Yield Stress		Ultimate Stress		Elongation %	Yield Strength	
			MPa	kpsi	MPa	kpsi		kN/m	lbs/in
Control	Polar Cap	Vertical	78.6	11.4	133.8	19.4	46	2.6	14.6
		Horizontal	80.0	11.6	131.0	19.0	54	2.3	13.1
	Equator	Vertical	84.8	12.3	135.8	19.7	73	3.2	18.5
		Horizontal	58.6	8.5	100.7	14.6	143	2.5	14.4
	1 cm up from base	Vertical	119.5	17.3	181.3	26.3	67	9.1	52.1
		Horizontal	46.9	6.8	54.5	7.9	338	3.7	21.0
5 months at D.S.E.T. (53,600 langleys)	Polar Cap	Vertical	95.1	13.8	97.2	14.1	40	2.6	15.2
		Horizontal	101.4	14.7	102.7	14.9	32	2.8	16.2
	Equator	Vertical	108.9	15.8	125.5	18.2	39	3.8	22.1
		Horizontal	71.7	10.4	84.8	12.3	94	2.3	13.5
	1 cm up from base	Vertical	128.2	18.6	161.3	23.4	61	8.1	46.5
		Horizontal	62.1	9.0	64.8	9.4	266	3.6	20.7

Table 7.2-4. Mechanical Properties of a Phase A Meliform Dome Before and After Desert Exposure

Exposure	Position	Direction	Yield Stress		Ultimate Stress		Elongation %	Yield Strength	
			MPa	kpsi	MPa	kpsi		kN/m	lbs/in
Control	Polar cap	Vertical	97.2	14.1	146.2	21.2	55	4.5	25.9
		Horizontal	90.3	13.1	161.3	23.4	68	4.2	24.0
	Equator	Vertical	95.1	13.8	144.8	21.0	144	5.7	32.7
		Horizontal	84.8	12.3	143.4	20.8	103	4.6	26
	1 cm up from base	Vertical	144.8	21.0	191.7	27.8	51	14.4	82.5
		Horizontal	68.3	9.9	77.9	11.3	232	6.2	35.6
5 months at D.S.E.T. (53,600 langleys)	Polar cap	Vertical	99.3	14.4	124.8	18.1	49	3.7	21.6
		Horizontal	108.2	15.7	135.1	19.6	51	3.8	22.0
	Equator	Vertical	101.4	14.7	133.1	19.3	89	5.1	29.4
		Horizontal	84.8	12.3	114.5	16.6	110	4.5	25.8
	1 cm up from base	Vertical	109.6	15.9	156.5	22.7	72	8.0	46.1
		Horizontal	73.8	10.7	75.2	10.9	271	6.3	36.4

Table 7.2-5. Mechanical Properties of a Phase A Petra AXB Laminated 4-Ply Butt Joints

Material		Integrated solar spectrum cone angle $.59^{\circ}$	633 nm source			
			Cone angle			
			$.08^{\circ}$	$.14^{\circ}$	$.28^{\circ}$	$.59^{\circ}$
PETG 7821	Control	87.6	87.0	87.2	87.5	87.6
	As received	85.6	86.1	86.3	86.8	86.9
	Cleaned	87.1	88.2	88.3	89.0	89.8
Petra (one piece)	Control	86.5	87.4	87.4	88.0	88.3
	As received	85.0	86.4	86.4	86.8	86.9
	Cleaned	85.0	86.6	87.3	87.4	87.6
Petra (4 ply)	Control	85.6	87.5	84.0	85.8	86.0
	As received	81.7	81.2	82.0	83.1	84.1
	Cleaned	81.5	83.2	83.5	85.0	86.0
Meliform	Control	79.0	76.4	76.8	76.8	77.0
	As received	76.5	74.6	74.7	75.2	75.6
	Cleaned	79.0	76.5	76.9	77.2	77.4
Kynar	Control	88.7	86.8	87.3	87.9	89.3
Melinex	Control	83.7	86.0	86.5	87.2	87.5

Table 7.2-6. Transmittance of Dome Materials Exposed 5 Months (53,600 Langley) in Desert

material is cleaned finally by immersion into an ultra-sonic bath, then rinsed in distilled water and air dried. The loss of transmittance (measured at the polar cap) due to the effects of particulate accumulation ranged between 2.2% and 0.9% measured at a cone angle of 0.14° with a 633 nm wavelength. This is even more interesting in light of the fact that there was no measurable rainfall at D.S.E.T. during the last month of exposure. From visual observations made at D.S.E.T. before removal of the domes, no variation in accumulation could be detected from top to bottom and side to side.

8.0 FULL SCALE DOME CAPABILITY

The present study has proven the feasibility of forming domes with adequate strength, transmittance, and geometry. The scale-up from experimental domes in Phase A to the pre-production domes in Phase B has proven the facility concept and verified the scaling factors for the thermal and air flow requirements. These concepts and techniques can be applied to full scale one-piece dome fabrication with considerable confidence.

The facility concept utilized in Phase B was based on full scale dome requirements. The base fixture was fixed, with the preheater being moveable. This allowed the film to be stationary during preheating and blowing. The moveable preheater worked very adequately. The movement time, 2 or 3 seconds, did not effect the forming cycle.

The infrared preheaters used in Phase B can be scaled up by a simple increase in area. The edge overlap and the variable heights designed into the facility are directly applicable to a full scale dome. An indication of the power output and time of preheating is shown in Table 8.0-1. These are the values used in all of the satisfactory domes that were formed.

Table 8.0-1. Preform Heating

<u>Power Source</u>	<u>Source Temp</u>	<u>Power Output</u>	<u>Heating Time</u>	
			<u>Kynar</u>	<u>Polyester</u>
Phase A/Tungsten Bulb	3000°C	5.4 kw/m ²	5 min.	3.5 min.
Phase B/I.R. Heater	370°C	10.8 kw/m ²	2.5 min.	-
Phase B/I.R. Heater	260°C	7.8 kw/m ²	-	1.2 min.

Domes formed at average strain rates of around 500%/minute were found to be satisfactory in both Phases A and B. To obtain this strain rate with the Phase B domes required flow rates of 5.1 m³/min (180 cfm). The maximum pressure required was 16.5 kPa (2.4 psi). Using this same strain rate for full scale domes will require flow rates of 1360 m³/min (48,000 cfm). The maximum pressures required would be about 2.1 kPa (0.3 psi).

The auxiliary heaters and the enclosure prevent premature or uneven cooling during forming of the dome. With the rapid forming cycle being used, this was minimized to a great extent in Phase B. For full scale dome fabrication an enclosure with auxiliary heating will be required that will minimize uneven radiant cooling during forming.

As the size of the preform becomes larger, more consideration must be given to holding techniques. Thermal expansion and uneven heating due to local heat sink areas are two of the prime problems. These problems were solved fairly satisfactorily in Phase B by maintaining a slight pressure on the preform during heating. For a full scale preform a comparable system could be used, or the material could be allowed to sag.

As discussed in Section 6.4, techniques for fabricating preforms for full scale domes have been developed. These consist of laminates and heat sealed joints. The most promising and cost effective technique for Kynar film is a pressed butt weld, which joins lengths of extruded material.

9.0 CONCLUSIONS AND RECOMMENDATIONS

The work in this study has proven the feasibility of using thermoforming techniques to fabricate one-piece domes. Experimental domes with adequate transmittance, strength and geometry have been made. High strain rates, (short forming times) and minimum forming temperature were found to be important to obtain high strength and acceptable shape.

Information was developed to allow scale-up to full size, 9.69 m (31.8 ft), diameter domes. Material preparation and initial thermoforming parameters were developed from two-directional stretching tests and from fabrication of 0.36 m (14 in) experimental domes. The facility concept and the thermal and blowing requirements were verified by forming 1.83 m (6 ft) diameter domes.

Processes were developed for fabricating preforms with heat seal joints, butt welded joints, and laminations. These techniques will allow an alternate to one-piece preforms where material widths or thicknesses are limited. Domes were formed using all of these methods. It is considered feasible to use these methods to form preforms 7.3 m (24 ft) in diameter for full scale dome fabrication.

Environmental testing included weatherometer tests and desert exposure tests. The weatherometer tests exposed Kynar and Tedlar samples to an equivalent 16 to 28 years exposure. The Kynar withstood the test much better than the Tedlar, losing only 2 to 5% of its transmittance compared to 50% for Tedlar. The first samples from the desert exposure test have been removed and tested after 5 months exposure. The unstabilized polyesters showed substantial degradation while the stabilized ones did not.

While it is considered that sufficient general information has been developed to proceed with full scale dome fabrication, there are areas where additional detailed information would be useful. This pertains primarily to preheating the Kynar preform. Studies on the absorption characteristics of Kynar, emitted energy characteristics of the heaters, thermal expansion effects of the preform, and heat sink potential of the preform holder would produce more efficient and uniform dome fabrication. This type of information would also be useful for polyester domes but it is not so critical due to the greater thermoforming temperature range for the polyesters.

DISTRIBUTION:

Foster-Miller Associates
135 Second Avenue
Waltham, MA 02154
Attn: Paul Tremblay

General Electric Company
P. O. Box 8661 - Room 7310
Philadelphia, PA 19101
Attn: R. Hobbs

Booz, Allen & Hamilton, Inc.
8801 E. Pleasant Valley Road
Cleveland, OH 44131
Attn: C. G. Howard

Solaramics, Inc.
1301 El Segundo Boulevard
El Segundo, CA 90245
Attn: H. E. Felix

General Electric
1 River Road
Schenectady, NY 12345
Attn: Richard Horton
John Garate
R. N. Griffin

Busche Energy Systems
7288 Murdy Circle
Huntington Beach, CA 92647
Attn: Ken Busche

Brookhaven National Laboratory
Upton, NY 11973
Attn: G. Cottingham

Aerospace Corporation
El Segundo Boulevard
El Segundo, CA 90274
Attn: Philip de Rienzo

McDonnell Douglas Astronautics
5301 Bolsa Avenue
Huntington Beach, CA 92647
Attn: R. L. Gervais
D. A. Steinmeyer

Martin Marietta Corporation
P. O. Box 179
Denver, CO 80201
Attn: T. R. Heaton
Lloyd Oldham

Northrup, Inc., Blake Laboratory
Suite 306
7061 S. University Boulevard
Littleton, CO 80122
Attn: Floyd Blake

Boeing Engineering & Construction
P. O. Box 3707
Seattle, WA 98124
Attn: Roger Gillette

Westinghouse Electric Corporation
Box 10864
Pittsburgh, PA 15236
Attn: J. J. Buggy

Northrup, Incorporated
302 Nichols Drive
Hutchins, TX 75141
Attn: J. A. Pietsch

Schumacher & Associates
2550 Fair Oaks Blvd., Suite 120
Sacramento, CA 95825
Attn: John C. Schumacher

Bechtel National Inc.
M/S 50/16
P. O. Box 3965
San Francisco, CA 94119
Attn: Ernie Lam

Ford Aerospace
3939 Fabian Way, T33
Palo Alto, CA 94303
Attn: Howard Sund

Veda, Inc.
400 N. Mobil, Bldg. D
Camarillo, CA 93010
Attn: Walter Moore

Pittsburgh Corning
800 Presque Isle Drive
Pittsburgh, PA 15239
Attn: David Rostoker

Springborn Laboratories
Water Street
Enfield, CT 06082
Attn: R. E. Cambron

Solar Energy Research Institute
1536 Cole Boulevard
Golden, CO 80401
Attn: Barry Butler
Dennis Horgan
John Thornton

Electric Power Research Institute
P. O. Box 10412
Palo Alto, CA 93403
Attn: John Bigger

Aerospace Corporation
Solar Thermal Projects
Energy Systems Group
P. O. Box 92957
Los Angeles, CA 90009
Attn: Elliott L. Katz

M. U. Gutstein, DOE/HQ
G. M. Kaplan, DOE/HQ
L. Melamed, DOE/HQ
J. E. Rannels, DOE/HQ
S. D. Elliott, DOE/SAN
R. N. Schweinberg, DOE/STMPO

Sandia Albuquerque:
C. N. Vittitoe, 4231
G. E. Brandvold, 4713
T. A. Dellin, 4723
J. A. Leonard, 4725
L. H. Harrah, 5811
R. B. Pettit, 5842
F. P. Gerstle, 5844

Sandia Livermore:

T. S. Gold, 8320
P. J. Eicker, 8326
P. L. Mattern, 8342
H. R. Sheppard, 8424
R. C. Wayne, 8450
W. G. Wilson, 8451 (10)
T. D. Brumleve, 8451

W. R. Delameter, 8451
C. L. Mavis, 8451
H. F. Norris, Jr., 8451
S. G. Peglow, 8451
C. J. Pignolet, 8451
A. C. Skinrod, 8452
J. D. Gilson, 8453

Technical Publications and Art Division, 8265 for TIC (27)
F. J. Cupps, 8265/Technical Library Processes Division, 3141
Technical Library Processes Division, 3141 (2)
Library and Security Classification Division, 8266-2 (3)